Closed-Form Exact and Asymptotic Expressions for the Symbol Error Rate and Capacity of the H-Function Fading Channel

Husam R. Alhennawi, Moataz M. H. El Ayadi, *Member, IEEE*,
Mahmoud H. Ismail, *Senior Member, IEEE*, and Hebat-Allah M. Mourad

***Abstract*—In this paper, we derive *closed-form exact* and *asymptotic* expressions for the symbol error rate (SER) and channel capacity when communicating over Fox's H-function fading channel. The SER expressions are obtained for numerous practically employed modulation schemes in case of single-branch and three multiple-branch diversity receivers: maximal ratio combining (MRC), equal gain combining (EGC), and selection combining (SC). The derived exact expressions are given in terms of the univariate and multivariate Fox's H-functions for which we provide a portable and efficient Python code. Since Fox's H-function fading channel represents the most generalized fading model ever presented in the literature, the derived expressions subsume most of those previously presented for all the known simple and composite fading models. Moreover, easy-to-compute asymptotic expansions are provided to easily study the behavior of the SER and channel capacity at high values of the average signal-to-noise ratio (SNR). The asymptotic expansions are also useful in comparing different modulation schemes and receiver diversity combiners. Numerical and simulation results are also provided to support the mathematical analysis and prove the validity of the obtained expressions.**

***Index Terms*—Asymptotic analysis, channel capacity, diversity systems, Fox's H-distribution, symbol error rate (SER).**

I. Introduction

PERFORMANCE evaluation of wireless communication systems over fading channels has always been an active area of research in the communication theory literature. Typically, performance metrics such as the bit/symbol error rates (BER/SER), outage probability, amount of fading (AoF), and ergodic channel capacity are usually used, among many others (see [1] and references therein). These quantities are of interest for both the single- and multiple-branch diversity receivers usually employed to reduce the detrimental effect of fading.

Manuscript received September 5, 2014; revised March 7, 2015; accepted April 3, 2015. Date of publication April 20, 2015; date of current version April 14, 2016. The review of this paper was coordinated by Dr. T. Jiang.

H. R. Alhennawi and H.-A. M. Mourad are with the Department of Electronics and Electrical Communications Engineering, Faculty of Engineering, Cairo University, Giza 12613, Egypt.

M. M. H. El Ayadi is with the Department of Engineering Mathematics and Physics, Faculty of Engineering, Cairo University, Giza 12613, Egypt (e-mail: moataz@eng.cu.edu.eg).

M. H. Ismail is with the Department of Electronics and Electrical Communications Engineering, Faculty of Engineering, Cairo University, Giza 12613, Egypt, and also with the Department of Electrical Engineering, American University of Sharjah, PO Box 26666, Sharjah, UAE (e-mail: mismail@eece.cu.edu.eg).

Color versions of one or more of the figures in this paper are available online at http://ieeexplore.ieee.org.

Digital Object Identifier 10.1109/TVT.2015.2424591

Over the past few years, numerous new fading models have been proposed to model either the fading or the joint shadowing/fading phenomena. These models generally provide a better fit for experimental data than the classical Rayleigh, Nakagami-m, and Rician ones. This is particularly true as new communication technologies are continuously being introduced and analyzed, for example, millimeter-wave communications, free-space optical (FSO) communications, and cognitive radios. Examples of these new models include the α–μ [2], the K [3], the generalized K [4], the extended generalized K (EGK) [5], the Gamma–Gamma [6] and the Málaga distributions [7], among many others. Having said that, the need for a unified fading model that subsumes most, if not all, of the proposed fading models to date and provides enough flexibility to accommodate future experimental results becomes eminent. One possible model that achieves these goals is the Fox's H-function fading model. Historically, the Fox's H-function distribution has been reported in mathematical publications as old as [8] and [9]. In these works, the Fox's H-function was introduced as a generalization for most of the probability distributions having a nonnegative support. In the context of wireless communications, since the received signal envelope and the signal-to-noise ratio (SNR) are always nonnegative, this distribution is very well suited to represent the probability density function (pdf) of the received signal envelope or SNR. Moreover, it was shown that the products, quotients, and powers of H-function variates are actually H-function variates themselves [8] and that the sum of H-function variates is indeed another H-function variate [10] (These properties are collectively known as the H-preserving property). This provides a very powerful tool to analyze diversity receivers and scenarios where mixed fading models are encountered, e.g., communications in presence of cochannel interference or within networks of relays. We can think of the Fox's H-function model as a "cast" that can be used to carry out a unified mathematical analysis for all possible fading models. More importantly, Fox's H-function model could be used to provide a possible fit for channel measurements that the current models fail to accommodate because of the multiple degrees of freedom that it offers.

Two important metrics that are usually used to characterize digital communications over fading channels are the SER/BER and the ergodic capacity [1]. In the same time, they are usually very challenging to obtain, particularly in closed form. This is particularly true for the considered Fox's H-function distribution. Unfortunately, the straightforward way, based on averaging the conditional probability of error on a specific SNR over the distribution of the SNR, rarely results in tractable integrals that lead to closed-form expressions. Hence, it has been limited to simple fading models such as the Rayleigh distribution. Alternatively, one of the most popular approaches is presented in the seminal works by Alouini *et al.* in [11] and [12], who have laid the foundation of what is commonly known as the moment-generating function (MGF) approach. This approach has been successfully applied to the Rayleigh, the Nakagami-m, the Rician, the Nakagami-q, and many other fading models (see [1, Ch. 8] and references therein). However, this approach requires performing some tricky integrations for moderately complicated fading distributions such as the case of Nakagami-m. That is why the literature is full of works that propose efficient techniques for numerically evaluating the performance using the MGF approach, particularly with diversity reception over some generalized fading channels (e.g., [13] and [14]). For complicated models such as the Fox's H-function distribution or even some of its special cases, e.g., the EGK and the Gamma–Gamma distributions, the MGF is actually given in the form of a Fox-H function, which limits the usability of the MGF approach. Additionally, the MGF approach cannot be straightforwardly used to estimate the asymptotic behavior of the SER for large values of the average SNR, which is an alternative simpler useful metric for performance evaluation.

Recently, in [15], we proposed a unified approach for calculating the SER of $\alpha{-}\mu$ fading channels based on the use of Mellin transform to express the SER in the form of a Mellin–Barnes integral [16], which can then be represented in terms of Fox's H-function in a direct manner. Depending on the specific parameter settings of the fading distribution and/or the modulation scheme, the obtained expressions can even be further simplified to simpler special functions such as Meijer's G-function or the hypergeometric function. Moreover, this approach enables obtaining asymptotic expansions that could be straightforwardly derived by evaluating some complex residues of the integrand function in the obtained Mellin–Barnes integral. Motivated by the successful application of this approach for $\alpha{-}\mu$ distribution in our work in [15], in this paper, we generalize our approach to deal with more generalized fading distributions and diversity receivers scenarios. In particular, we extend the previous work in [15] in the following ways.

1) We derive novel closed-form expressions for the SER of most (if not all) of the practically used modulation schemes when operating over Fox's H-function fading channel in presence of additive white Gaussian noise (AWGN). This generalization is not trivial because, unlike the $\alpha{-}\mu$ distribution, we have to derive the necessary conditions on Fox's H-function distribution parameters so that the SNR distribution is valid mathematically. Moreover, the asymptotic expansions, which we do believe are of prime importance practically, require more analysis and in some cases further approximations.
2) We present a *unified* analysis framework to derive exact and asymptotic expressions for the SER of a wide range of diversity receivers over Fox's H-function channel. While we focus in the current paper on the equal gain, maximal ratio, and selection combining (EGC, MRC, and SC, respectively) schemes, the analysis is directly applicable to other types of diversity receivers. Moreover, the SC was *not* addressed in the previous work. In addition, we also provide simple asymptotic expansions for the SER in these cases, which can be very easily and quickly computed, even for a large number of branches.
3) We extend our framework to accommodate the ergodic capacity calculations and apply it to Fox's H-function fading model assuming single-branch communications. Moreover, we derive the asymptotic expansion for the ergodic channel capacity and verify the results via simulations.
4) We present a portable implementation of the multivariate H-function using Python in Appendix A. The code is efficient and provides very accurate results. Its execution time for up to four branches does not exceed a few seconds. To the best of the authors' knowledge, this is a new contribution to the literature of digital communications.

To the best of the authors' knowledge, our results represent the most general SER and capacity expressions ever presented in the literature for communications over fading channels and subsume most of those previously presented in the literature for the classical and more recent fading models alike, whether simple or composite. More importantly, the presented framework enables us to derive straightforwardly derive easy-to-calculate asymptotic expansions, which do serve as very accurate approximations of the SER and the ergodic capacity for high average SNR values. This is verified in many different cases as illustrated in the simulations. Moreover, and unlike the exact expressions, they help to easily compare the performance over different fading channels (which are special cases of the Fox's H-function model), for different modulation schemes and diversity combining strategies.

It is worth mentioning here that the use of Fox's H-function as a unified model for fading statistics is not in fact new. In [17], Fox's H-function model was used to characterize the spherically invariant random process, a generalization of the Gaussian process, which can be used to provide a unified theory to model fading channel statistics. In [18], unified expressions for the effective capacity of fading channels under a quality-of-service constraint were obtained through the use of Fox's H-function distribution. Moreover, in [19], a variation of Fox's H-function fading model presented here, which consists of a summation of multiple Fox's H-functions (titled as the hyper Fox's H-function), was discussed. The main differences between this work and the one at hand are as follows. First, [19] only considers the BER for two binary modulation schemes, namely, binary frequency-shift keying and binary phase-shift keying (BFSK and BPSK, respectively). In this paper, however, we manage to obtain closed-form exact and asymptotic expressions for the SER for M-ary PSK, M-QAM, M-ASK, as well as noncoherent M-ary FSK (NC M-ary FSK). Second, [19] only considers MRC as an example for diversity reception while we consider EGC, MRC, and SC as mentioned earlier. It is worth mentioning that the model in [19] might seem more general than the one presented here since it involves a summation of multiple Fox's H-functions and not just one, which enables it to subsume a few more fading models as special cases, e.g., the hyper-gamma [20]. However, the results presented herein can be straightforwardly extended to follow the model in [19] since all the operations involved are linear.

The remainder of this paper is organized as follows. Section II treats the single-branch receivers and derives closed-form SER and capacity expressions as well as asymptotic expansions assuming Fox's H-function fading model. Several special cases are also presented, and their expressions are compared against those previously published in the literature. In Section III, the analysis is extended to the multiple-branch EGC, MRC, and SC diversity receivers. Numerical and simulation results are then presented in Section IV before this paper is finally concluded in Section V.

II. Single-Branch Communication

We consider communications over a fading channel where the SNR γ follows the unified Fox's H-function distribution for which the pdf is given by [8, Sec. 4.1]:

$$f_\gamma(\gamma) = \kappa H_{p,q}^{m,n}\left(\lambda\gamma \middle| \begin{matrix} (a_j, A_j)_{j=1:p} \\ (b_j, B_j)_{j=1:q} \end{matrix}\right), \quad \gamma > 0 \tag{1}$$

where $\lambda > 0$ and the constant κ are such that $\int_0^\infty f_\gamma(\gamma)d\gamma = 1$. The notation $(x_j, y_j)_{j=1:\ell}$ is a shorthand for $(x_1, y_1), \ldots, (x_\ell, y_\ell)$. The univariate H-function, $H_{p,q}^{m,n}(\zeta)$, is defined by [21]

$$H_{p,q}^{m,n}\left(\zeta \middle| \begin{matrix} (a_j, A_j)_{j=1:p} \\ (b_j, B_j)_{j=1:q} \end{matrix}\right) = \frac{1}{2\pi i} \times \int_{\mathcal{L}} \frac{\prod_{j=1}^{m} \Gamma(b_j + B_j s) \prod_{j=1}^{n} \Gamma(1 - a_j - A_j s)}{\prod_{j=n+1}^{p} \Gamma(a_j + A_j s) \prod_{j=m+1}^{q} \Gamma(1 - b_j - B_j s)} \zeta^{-s} ds \tag{2}$$

where $A_j > 0$ for all $j = 1, \ldots, p$, and $B_j > 0$ for all $j = 1, \ldots, q$ and the path of the integration $\mathcal{L}$ depends on the value of the parameters. Examples of how classical and more recent fading models can fit into this unified fading model are provided in [19, Tab. II–V]. As mentioned earlier, some of these fading models need to be approximated by a summation of Fox's H-functions. The model presented in (1) can be easily extended to accommodate these cases. We chose, however, to work with a single Fox's H-function to keep the presentation as compact as possible. Some other fading models that are not mentioned in [19, Tab. II–V] but can still be considered special cases of the Fox's H-function fading model are the Málaga and the gamma–gamma (double gamma). We illustrate this fact in Appendix B. Here, we seek to derive exact expressions as well as asymptotic expansions for the SER and the channel capacity. For the validity of our analysis, we require that $f_\gamma(\gamma)$ be a valid pdf and have a Mellin transform. Therefore, in Section II-A, we derive the sufficient conditions for that to happen. SER analysis is presented in Section II-B followed by channel capacity analysis in Section II-C.

A. *Sufficient Conditions for the Validity of the Analysis*

Our previously proposed SER calculation framework in [15] was completely dependent on the straightforward and simple derivation of the Mellin transform of $f_\gamma(\gamma)$. For the general case of unified Fox's H-function distribution, the Mellin transform can be easily obtained only if the path of integration in (1) is a straight line parallel to the imaginary axis. Therefore, the following condition needs to be enforced [21]:

$$\sum_{j=1}^{n} A_j - \sum_{j=n+1}^{p} A_j + \sum_{j=1}^{m} B_j - \sum_{j=m+1}^{q} B_j > 0. \tag{3}$$

Fortunately, all the considered distributions in [19, Tab. II–V] satisfy this requirement. In fact, in all of them, $n = p = 0$, and $m = q$. Moreover, as required by the definition of the H-function, the poles of the factors $\Gamma(b_j + B_j s)$, $j = 1, \ldots, m$, should be separable from those of $\Gamma(1 - a_j - A_j s)$, $j = 1, \ldots, n$. This is equivalent to having $l < u$, where $l = -\min_{j=1,\ldots,m}(\Re\{b_j/B_j\})$, $u = \min_{j=1,\ldots,n}(\Re\{1 - a_j/A_j\})$, and $\Re\{\cdot\}$ denotes the real part of a complex quantity. In such a case, it can be shown that the path of integration can be taken as a straight line from $\sigma - i\infty$ to $\sigma + i\infty$, where σ satisfies $l < \sigma < u$.

Now, in order for $f_\gamma(\gamma)$ to be a valid pdf, its integration from 0 to ∞ needs to be equal to one. At this point, it is more convenient to start working with the Mellin transform of $f_\gamma(\gamma)$ rather than the distribution itself. This is, in fact, one of the major strengths of the unified Fox's H-function fading model; its Mellin transform is straightforward to obtain and easy to deal with. The Mellin transform of a continuous function is defined as [22]

$$f^*(s) \equiv \mathcal{M}\{f(\gamma)\} = \int_0^\infty f(\gamma)\gamma^{s-1} d\gamma. \tag{4}$$

The aforementioned condition is now equivalent to having the point $s = 1$ in the region of convergence (ROC) of $f^*(s)$ since $f^*(1) = \int_{\gamma=0}^\infty f_\gamma(\gamma)\gamma^{1-1} d\gamma = 1$. That is, we must have $l < 1 < u$. An illustration of this condition is shown in Fig. 1(a). This condition is again satisfied by all the distributions investigated in [19, Tab. II–V]. Finally, to have a finite value for κ, $\lim_{s\to 1} f^*(s)$ must exist and be equal to 1. From (1) and (4), the Mellin transform of $f_\gamma(\gamma)$ can be obtained directly using [21, Eq. (2.8)] as

$$f^*(s) = \kappa\lambda^{-s} \frac{\prod_{j=1}^{m} \Gamma(b_j + B_j s) \prod_{j=1}^{n} \Gamma(1 - a_j - A_j s)}{\prod_{j=n+1}^{p} \Gamma(a_j + A_j s) \prod_{j=m+1}^{q} \Gamma(1 - b_j - B_j s)}. \tag{5}$$

Hence, we do require that the following limit exist and be bounded:

$$\frac{\kappa}{\lambda} = \lim_{s\to 1} \frac{\prod_{j=n+1}^{p} \Gamma(a_j + A_j s) \prod_{j=m+1}^{q} \Gamma(1 - b_j - B_j s)}{\prod_{j=1}^{m} \Gamma(b_j + B_j s) \prod_{j=1}^{n} \Gamma(1 - a_j - A_j s)}. \tag{6}$$

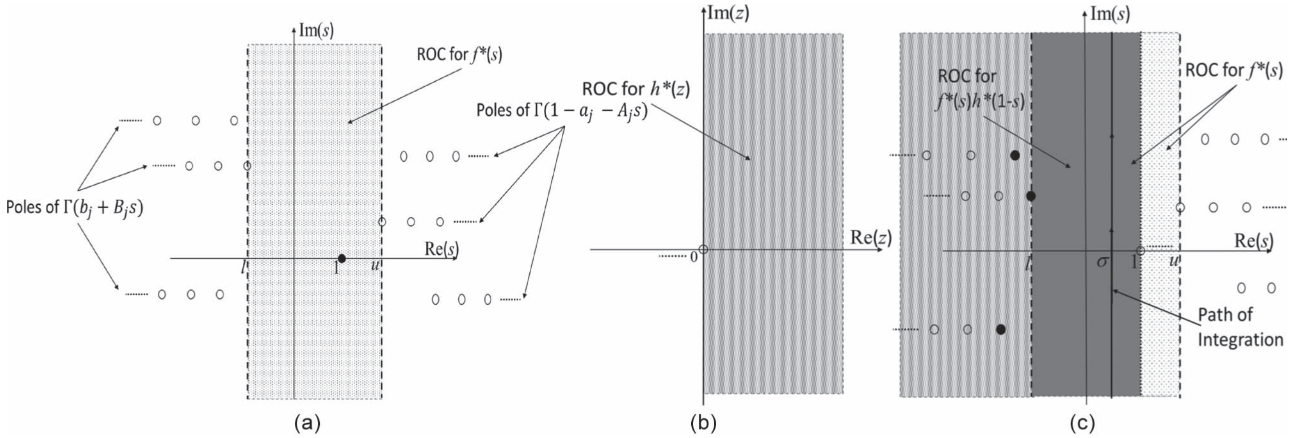

Fig. 1. (a) ROC of $f^*(s)$. Note that the point $s=1$ must be inside the ROC because $f_\gamma(\gamma)$ is a pdf. In this example, $m=n=3$. (b) ROC of $h^*(z)$ in the z-domain. (c) Intersection of the ROCs of $f^*(s)$ and $h^*(1-s)$ is the solid gray region $l < \Re\{s\} < 1$. The solid circles refer to the poles considered for deriving the asymptotic expansion of the SER.

TABLE I

BASIC COMPONENTS OF $h(\gamma)$ TOGETHER WITH THEIR MELLIN TRANSFORMS

$h_r(\gamma;\theta)$	Mellin transform	Modulation schemes
$h_0(\gamma;\mathrm{b}) = e^{-\mathrm{b}\gamma}$	$h_0^*(s;\mathrm{b}) = \mathrm{b}^{-s}\Gamma(s)$	DBPSK, NC M-FSK
$h_1(\gamma;\mathrm{b}) = \int_{u=\gamma}^{\infty} u^{-1/2}e^{-\mathrm{b}u}du$	$h_1^*(s;\mathrm{b}) = s^{-1}\mathrm{b}^{-s-1/2}\Gamma(s+1/2)$	CBPSK, CBFSK, M-PSK, M-QAM
$h_2(\gamma;\mathrm{a},\mathrm{b}) = \int_{u=\gamma}^{\infty} u^{-1/2}e^{-\mathrm{b}u}Q'(\sqrt{\mathrm{a}u})du$	$h_2^*(s;\mathrm{a},\mathrm{b}) = \frac{\mathrm{b}^{-s}}{2s\sqrt{\mathrm{b}\pi}} \times \frac{1}{2\pi i}\int_{w=c_2-i\infty}^{c_2+i\infty} \frac{\Gamma(1/2-w)\Gamma(s+w+1/2)}{w}\left(\frac{\mathrm{a}}{2\mathrm{b}}\right)^w dw$	PSK, QAM

B. Symbol-Error-Rate Analysis

1) Exact Expressions: The derivation here is based on [15, Th. I], which we proved earlier. We recall this theorem here for convenience.

Theorem 1: Consider a general fading channel where the received SNR pdf is $f_\gamma(\gamma)$ having a Mellin transform $f^*(s)$. If the Mellin transform of $P(\text{error}|\gamma)$ exists, then the unconditional SER for a single-branch receiver is given by

$$P_e = \frac{1}{2\pi i}\int_{\sigma-i\infty}^{\sigma+i\infty} f^*(s)h^*(1-s)ds \tag{7}$$

where $h^*(s)$ is the Mellin transform of $h(\gamma) \equiv P(\text{error}|\gamma)$, and the constant σ is such that σ lies in the ROC of both $f^*(s)$ and $h^*(1-s)$.

From [1, Ch. 8], it is not difficult to observe that the conditional SER expression $h(\gamma)$ for each of the aforementioned modulation schemes is a linear combination of one or more of the terms $h_0(\gamma;\mathrm{b})$, $h_1(\gamma;\mathrm{b})$, and $h_2(\gamma;\mathrm{a},\mathrm{b})$ listed in the first column of Table I. It is straightforward to prove that the ROC of their Mellin transforms, presented in the second column of the table using (4) along with the definition of the Gamma function, is $\Re\{s\} > 0$. Hence, the ROC of $h^*(1-s)$ in (7) is $\Re\{s\} < 1$. Intersecting that ROC with the ROC of $f^*(s)$, we easily conclude that one needs to have $l < \sigma < 1$ in order for (7) to be valid. This result is shown in Fig. 1(b) and (c). Now, according to (7) and the fact that $h(\gamma)$ is a linear combination of one or more of the functions mentioned earlier, it can be easily shown that the SER itself is a linear combination of one or more of the functions, i.e.,

$$\mathcal{I}_r(\theta) \equiv \frac{1}{2\pi i}\int_{\sigma-i\infty}^{\sigma+i\infty} f^*(s)h_r^*(1-s;\theta)ds, \quad r = 0, 1 \text{ and } 2 \tag{8}$$

where $\theta = \{\mathrm{b}\}$ for $r = 0, 1$ and $\theta = \{\mathrm{a},\mathrm{b}\}$ for $r = 2$, which we refer to as the basic functions. For $\mathcal{I}_0(\mathrm{b})$, we have $h_0^*(s;\mathrm{b}) = \mathrm{b}^{-s}\Gamma(s)$ from Table I. Substituting from (5) into (8) and using $h_0^*(1-s;\mathrm{b}) = \mathrm{b}^{s-1}\Gamma(1-s)$ and $\theta = \mathrm{b}$, we easily get the result in (9), shown at the bottom of the page.

Following similar steps, one can derive similar expressions for $\mathcal{I}_1(\mathrm{b})$ and $\mathcal{I}_2(\mathrm{a},\mathrm{b})$. Now, referring to the definition of the H-function in (2) and using the relation [21, Eq. (1.60)] so as the results include the ratio κ/λ for convenience, the results for $\mathcal{I}_r(\theta)$, $r = 0, 1, 2$, which is shown in (10), at the bottom of the next page, follow immediately. In these expressions,

$$\mathcal{I}_0(\mathrm{b}) = \frac{\kappa}{\mathrm{b}}\frac{1}{2\pi i}\int_{\sigma-i\infty}^{\sigma+i\infty} \frac{\left(\prod_{j=1}^{m}\Gamma\left(b_j+B_js\right)\right)\Gamma(1-s)\prod_{j=1}^{n}\Gamma\left(1-a_j-A_js\right)}{\prod_{j=n+1}^{p}\Gamma\left(a_j+A_js\right)\prod_{j=m+1}^{q}\Gamma\left(1-b_j-B_js\right)}\left(\frac{\lambda}{\mathrm{b}}\right)^{-s}ds \tag{9}$$

TABLE II
FINAL FORM OF THE P_e FOR THE DIFFERENT MODULATION SCHEMES WITH FOX'S H-FUNCTION FADING

Modulation Scheme	P_e
CBFSK	$\frac{\kappa/\lambda}{2\sqrt{\pi}} H^{m,n+2}_{p+2,q+1}\left(2\lambda \middle\vert \begin{matrix} (1,1),(\frac{1}{2},1),(a_j+A_j,A_j)_{j=1:p} \\ (b_j+B_j,B_j)_{j=1:q},(0,1) \end{matrix}\right)$
M-ary ASK	$\frac{(M-1)(\kappa/\lambda)}{M\sqrt{\pi}} H^{m,n+2}_{p+2,q+1}\left(\frac{M^2-1}{3}\lambda \middle\vert \begin{matrix} (1,1),(\frac{1}{2},1),(a_j+A_j,A_j)_{j=1:p} \\ (b_j+B_j,B_j)_{j=1:q},(0,1) \end{matrix}\right)$
M-ary PSK	$\frac{\kappa/\lambda}{2\sqrt{\pi}}\left[H^{m,n+2}_{p+2,q+1}\left(\frac{\lambda}{\sin^2(\pi/M)} \middle\vert \begin{matrix} (1,1),(\frac{1}{2},1),(a_j+A_j,A_j)_{j=1:p} \\ (b_j+B_j,B_j)_{j=1:q},(0,1) \end{matrix}\right) + \frac{1}{\sqrt{\pi}} H^{0,1;1,1;m,n+1}_{1,0;1,2;p+1,q+1}\left(\cot^2\left(\frac{\pi}{M}\right), \frac{\lambda}{\sin^2(\pi/M)} \middle\vert \begin{matrix} (\frac{1}{2};1,1) & (1,1) & (1,1),(a_j+A_j,A_j)_{j=1:p} \\ - & (\frac{1}{2},1),(0,1) & (b_j+B_j,B_j)_{j=1:q},(0,1) \end{matrix}\right)\right]$
M-QAM	$\frac{2(\sqrt{M}-1)(\kappa/\lambda)}{M\sqrt{\pi}}\left[H^{m,n+2}_{p+2,q+1}\left(\frac{2(M-1)\lambda}{3} \middle\vert \begin{matrix} (1,1),(\frac{1}{2},1),(a_j+A_j,A_j)_{j=1:p} \\ (b_j+B_j,B_j)_{j=1:q},(0,1) \end{matrix}\right) + \frac{\sqrt{M}-1}{\sqrt{\pi}} H^{0,1;1,1;m,n+1}_{1,0;1,2;p+1,q+1}\left(\cot^2\left(\frac{\pi}{M}\right), \frac{2(M-1)\lambda}{3} \middle\vert \begin{matrix} (\frac{1}{2};1,1) & (1,1) & (1,1),(a_j+A_j,A_j)_{j=1:p} \\ - & (\frac{1}{2},1),(0,1) & (b_j+B_j,B_j)_{j=1:q},(0,1) \end{matrix}\right)\right]$
DBPSK	$\frac{\kappa/\lambda}{2} H^{m,n+1}_{p+1,q}\left(\lambda \middle\vert \begin{matrix} (1,1),(a_j+A_j,A_j)_{j=1:p} \\ (b_j+B_j,B_j)_{j=1:q} \end{matrix}\right)$
NC M-ary FSK	$\frac{\kappa}{\lambda}\sum_{n=1}^{M-1}(-1)^{n+1}\binom{M-1}{n}\frac{1}{n+1} H^{m,n+1}_{p+1,q}\left(\frac{(n+1)\lambda}{n} \middle\vert \begin{matrix} (1,1),(a_j+A_j,A_j)_{j=1:p} \\ (b_j+B_j,B_j)_{j=1:q} \end{matrix}\right)$

$H^{0,n;m_1,n_1,\ldots,m_L,n_L}_{p,q;p_1,q_1,\ldots,p_L,q_L}(\zeta_1,\ldots,\zeta_L)$ is the multivariate H-function defined by [21, Eq. (A.1)]. Finally, the SER can be obtained by substituting the expressions in (10), shown at the bottom of the page, into the expressions in [15, Tab. III], yielding the final forms provided in Table II. We want to stress here that these expressions are, to the best of the authors' knowledge, the most general SER expressions ever presented in the literature. They literally subsume each and every SER expression previously presented as a special case.

2) Asymptotic Expansions: In many practical settings, the obtained exact expressions could be of limited value because of the difficulty encountered in evaluating the univariate and multivariate H-functions. Generally, the H-function is given in the form of a complex integral, which is computed numerically. For high values of the average SNR, the exact value of the SER is very small; thus, their computation using numerical integration methods is subject to underflow. Therefore, it is often desired to derive simpler asymptotic expansions of the SER for large values of the average SNR, which is a typical case of many practical situations. In addition to their simplicity of computations, asymptotic expansions offer an indication of the rate of change of the SER with respect to the SNR. This is very useful in comparing different modulation schemes/fading channels. Moreover, their logarithms can be computed efficiently; hence, their computation is not subject to underflow. Taking a careful look at [19, Tab. II–V], we notice that the multiplier λ is usually inversely proportional to the average SNR. Therefore, asymptotic expansions should be derived in terms of positive powers of λ. This could be accomplished by evaluating the complex residues of the functions $\mathcal{I}_r(\theta)$ at the *largest negative poles* of the terms $\Gamma(b_j+B_js)$, $j=1,\ldots,m$. That is, we should consider the poles given by $s=-b_j/B_j$, $j=1,\ldots,m$, indicated in Fig. 1(c) as solid circles. In fact, the asymptotic expansions of the H-function depend on the order of the poles. Therefore, we present the most general form based on [23, Th. 1.12], which we restate below after some slight modifications.

Theorem 2: Consider the H-function defined by (2), and let the condition (3) be satisfied. Define the set of unique poles $S=\{s_1,\ldots,s_{m'}\}$, where $s_j=-b_j/B_j$, and $m'\le m$. For each pole s_j, define the set of indexes $K_j=\{k: k\in\{1,\ldots,m\}, r_{k,j}=-b_k+B_kb_j/B_j\in\{0,1,2,\ldots\}\}$, and let $N_j=|K_j|$ be the multiplicity of the pole $s_j=-b_j/B_j$. The asymptotic expansion near $\zeta=0$ is given by

$$H^{m,n}_{p,q}(\zeta)\sim\sum_{j=1}^{m'}E_j\left[-\ln(\zeta)\right]^{N_j-1}\zeta^{\frac{-b_j}{B_j}} \tag{11}$$

where the constants E_j, $j=1,\ldots,m'$ are given by (12),

$$E_j=\frac{1}{(N_j-1)!}\times\prod_{k\in K_j}\frac{(-1)^{r_{k,j}}}{r_{k,j}!B_k} \times\frac{\prod\limits_{k\notin K_j}\Gamma\left(b_k-B_k\frac{b_j}{B_j}\right)\prod\limits_{k=1}^{n}\Gamma\left(1-a_k+A_k\frac{b_j}{B_j}\right)}{\prod\limits_{k=n+1}^{p}\Gamma\left(a_k-A_k\frac{b_j}{B_j}\right)\prod\limits_{k=m+1}^{q}\Gamma\left(1-b_k+B_k\frac{b_j}{B_j}\right)} \tag{12}$$

$$\mathcal{I}_0(\mathrm{b})=\frac{\kappa}{\lambda}H^{m,n+1}_{p+1,q}\left(\frac{\lambda}{\mathrm{b}}\middle\vert\begin{matrix}(1,1),(a_j+A_j,A_j)_{j=1:p}\\(b_j+B_j,B_j)_{j=1:q}\end{matrix}\right) \tag{10a}$$

$$\mathcal{I}_1(\mathrm{b})=\frac{\frac{\kappa}{\lambda}}{\sqrt{\mathrm{b}}}H^{m,n+2}_{p+2,q+1}\left(\frac{\lambda}{\mathrm{b}}\middle\vert\begin{matrix}(1,1),\left(\frac{1}{2},1\right),(a_j+A_j,A_j)_{j=1:p}\\(b_j+B_j,B_j)_{j=1:q},(0,1)\end{matrix}\right) \tag{10b}$$

$$\mathcal{I}_2(\mathrm{a},\mathrm{b})=\frac{\frac{\kappa}{\lambda}}{2\sqrt{\pi}\mathrm{b}^{\frac{1}{2}}}H^{0,1;1,1;m,n+1}_{1,0;1,2;p+1,q+1}\left(\frac{\mathrm{a}}{2\mathrm{b}},\frac{\lambda}{\mathrm{b}}\middle\vert\begin{matrix}\left(\frac{1}{2};1,1\right) & (1,1) & (1,1),(a_j+A_j,A_j)_{j=1:p}\\ - & \left(\frac{1}{2},1\right),(0,1) & (b_j+B_j,B_j)_{j=1:q},(0,1)\end{matrix}\right) \tag{10c}$$

TABLE III
ASYMPTOTIC EXPRESSIONS FOR P_e FOR THE DIFFERENT MODULATION SCHEMES OVER FOX'S H-FUNCTION FADING. E_j, N_j, AND m' ARE AS DEFINED IN THEOREM 2

Modulation Scheme	Asymptotic P_e
CBFSK	$\frac{\kappa/\lambda}{2\sqrt{\pi}}\sum_{j=1}^{m'}\frac{E_j}{1+b_j/B_j}\Gamma\left(\frac{3}{2}+\frac{b_j}{B_j}\right)\left[-\ln(2\lambda)\right]^{N_j-1}(2\lambda)^{\frac{b_j}{B_j}+1}$
M-ary ASK	$\frac{(M-1)(\kappa/\lambda)}{M\sqrt{\pi}}\sum_{j=1}^{m'}\frac{E_j}{1+b_j/B_j}\Gamma\left(\frac{3}{2}+\frac{b_j}{B_j}\right)\left[\ln\left(\frac{3}{(M^2-1)\lambda}\right)\right]^{N_j-1}\left(\frac{M^2-1}{3}\lambda\right)^{\frac{b_j}{B_j}+1}$
M-ary PSK	$\frac{\kappa/\lambda}{\sqrt{\pi}}\sum_{j=1}^{m'}\left\{\frac{E_j}{1+b_j/B_j}\left[\ln\left(\frac{\sin^2(\pi/M)}{\lambda}\right)\right]^{N_j-1}\left(\frac{\lambda}{\sin^2(\frac{\pi}{M})}\right)^{\frac{b_j}{B_j}+1}\times\left[\frac{1}{2}\Gamma\left(\frac{3}{2}+\frac{b_j}{B_j}\right)+\frac{\cot(\frac{\pi}{M})}{\sqrt{\pi}}\Gamma\left(2+\frac{b_j}{B_j}\right){}_2F_1\left(\frac{1}{2},2+\frac{b_j}{B_j};\frac{3}{2};-\cot^2\left(\frac{\pi}{M}\right)\right)\right]\right\}$
M-QAM	$\frac{2\kappa/\lambda}{\sqrt{\pi}}\frac{\sqrt{M}-1}{\sqrt{M}}\sum_{j=1}^{m'}\left\{\frac{E_j}{1+b_j/B_j}\left[\ln\left(\frac{3}{2(M-1)\lambda}\right)\right]^{N_j-1}\left(\frac{2(M-1)}{3}\lambda\right)^{\frac{b_j}{B_j}+1}\times\left[\frac{1}{\sqrt{M}}\Gamma\left(\frac{3}{2}+\frac{b_j}{B_j}\right)+2\frac{\sqrt{M}-1}{\sqrt{M\pi}}\Gamma\left(2+\frac{b_j}{B_j}\right){}_2F_1\left(\frac{1}{2},2+\frac{b_j}{B_j};\frac{3}{2};-1\right)\right]\right\}$
DBPSK	$\frac{\kappa/\lambda}{2}\sum_{j=1}^{m'}E_j\Gamma\left(1+\frac{b_j}{B_j}\right)\left[-\ln(\lambda)\right]^{N_j-1}(\lambda)^{\frac{b_j}{B_j}+1}$
NC M-ary FSK	$\frac{\kappa}{\lambda}\sum_{n=1}^{M-1}(-1)^{n+1}\binom{M-1}{n}\frac{1}{n+1}\sum_{j=1}^{m'}E_j\Gamma\left(1+\frac{b_j}{B_j}\right)\left[\ln\left(\frac{n}{(n+1)\lambda}\right)\right]^{N_j-1}\left(\frac{n+1}{n}\lambda\right)^{\frac{b_j}{B_j}+1}$

which simplifies for simple poles ($K_j=\{j\}$, $N_j=1$, and $r_{j,j}=0$) to the following expression:

$$E_j=\frac{1}{B_j}\frac{\prod_{\substack{k=1\\k\neq j}}^{m}\Gamma\left(b_k-B_k\frac{b_j}{B_j}\right)\prod_{k=1}^{n}\Gamma\left(1-a_k+A_k\frac{b_j}{B_j}\right)}{\prod_{k=n+1}^{p}\Gamma\left(a_k-A_k\frac{b_j}{B_j}\right)\prod_{k=m+1}^{q}\Gamma\left(1-b_k+B_k\frac{b_j}{B_j}\right)}. \tag{13}$$

Thus, the asymptotic expressions for the functions $\mathcal{I}_r(\theta)$ can be easily evaluated thanks to Theorem 2, yielding the results in (14). In these expressions, ${}_2F_1(\cdot,\cdot;\cdot;\cdot)$ is the Gauss hypergeometric function, κ/λ is given by (6), and E_j, N_j, and m' are given by Theorem 2. We should notice that, according to the second condition in Section II-A, we guarantee that all the powers $1+(b_j/B_j)$, $j=1,\ldots,m$, have positive real parts. Thus, we are confident that the obtained asymptotic expansions decrease monotonically with the increase in the average SNR. Similar to the case of exact expressions, asymptotic expansions of the SER for different modulation schemes are easily obtained by substituting from (14) into the expressions in [15, Tab. III], yielding the results in Table III.

$$\mathcal{I}_0(\mathrm{b})\sim\frac{\kappa}{\lambda}\sum_{j=1}^{m'}E_j\Gamma\left(1+\frac{b_j}{B_j}\right)\left[\ln\left(\frac{\mathrm{b}}{\lambda}\right)\right]^{N_j-1}\left(\frac{\lambda}{\mathrm{b}}\right)^{\frac{b_j}{B_j}+1} \tag{14a}$$

$$\mathcal{I}_1(\mathrm{b})\sim\frac{\kappa/\lambda}{\sqrt{\mathrm{b}}}\sum_{j=1}^{m'}\frac{E_j}{1+b_j/B_j}\Gamma\left(\frac{3}{2}+\frac{b_j}{B_j}\right)\times\left[\ln\left(\frac{\mathrm{b}}{\lambda}\right)\right]^{N_j-1}\left(\frac{\lambda}{\mathrm{b}}\right)^{\frac{b_j}{B_j}+1} \tag{14b}$$

$$\mathcal{I}_2(\mathrm{a},\mathrm{b})\sim\frac{(\kappa/\lambda)\sqrt{\mathrm{a}}}{\mathrm{b}\sqrt{2\pi}}\sum_{j=1}^{m'}\frac{E_j}{1+(b_j/B_j)}\Gamma\left(2+\frac{b_j}{B_j}\right)\times{}_2F_1\left(\frac{1}{2},2+\frac{b_j}{B_j};\frac{3}{2};-\frac{\mathrm{a}}{2\mathrm{b}}\right)\times\left[\ln\left(\frac{\mathrm{b}}{\lambda}\right)\right]^{N_j-1}\left(\frac{\lambda}{\mathrm{b}}\right)^{\frac{b_j}{B_j}+1} \tag{14c}$$

C. Channel Capacity

One of the main contributions of this paper is deriving closed-form exact and asymptotic expressions for the average ergodic capacity of the Fox's H-function fading channel based on our previously introduced framework. The capacity of a fading channel is given by

$$C=\int_{\gamma=0}^{\infty}f_\gamma(\gamma)\ln(1+\gamma)d\gamma \tag{15}$$

where we chose the natural logarithm in the given definition to simplify the analysis.[1]

1) Exact Expression: Using Parseval's relation for the Mellin transform [22, Eq. (2.31)], it can be easily shown that the capacity is given by

$$C=\frac{1}{2\pi i}\int_{\sigma-i\infty}^{\sigma+i\infty}f^*(s)c^*(1-s)ds \tag{16}$$

[1]It goes without saying that using the $\log_2(\cdot)$ function will just entail a scale factor to our results.

where $c^*(s)$ is the Mellin transform of $\ln(1+\gamma)$. Using [24, Eq. (17.43.23)] along with the gamma reflection formula [25, App. II.1], i.e., $\Gamma(s)\Gamma(1-s) = \pi/\sin(\pi s)$, it can be shown that $c^*(s)$ is given by

$$c^*(s) = -\Gamma(s)\Gamma(-s) = \frac{\Gamma(s+1)\Gamma(-s)}{-s}, \quad -1 < \Re\{s\} < 0. \tag{17}$$

Hence, the ROC of $c^*(1-s)$ is $1 < \Re\{s\} < 2$. Intersecting that ROC with that of $f^*(s)$, the integration (16) will be valid for $1 < \sigma < \min(2, u)$. Substituting from (17) and (5) into (16), employing the definition of the H-function and using [21, Eq. (1.60)], we obtain

$$C = \frac{\kappa}{\lambda} H^{m+2,n+1}_{p+2,q+2}\left(\lambda \middle| \begin{array}{c} (0,1),(a_j+A_j,A_j)_{j=1:p},(1,1) \\ (0,1),(0,1),(b_j+B_j,B_j)_{j=1:q} \end{array}\right). \tag{18}$$

2) Asymptotic Expansion: Since the integral in (16) converges for $1 < \sigma < \min(2, u)$, the asymptotic expansion is derived by evaluating the residues of this integral at the largest poles closest to the path of integration from the left. Basically, we have three sets of poles lying on the left of the integration path: a double pole at $s = 1$, the poles of $\Gamma(s)$ given by $s = 0, -1, \ldots$, and the poles of the terms $\Gamma(b_j + B_j s)$, $j = 1, \ldots, m$. For simplicity, we shall consider only the double pole at $s = 1$ because it is the closest to the integration path, and we believe that the obtained expansion upon considering only this pole is adequate for most applications. If more accurate expansions are required, the residues at the other poles, e.g., $s = -b_j/B_j$, $j = 1, \ldots, m$ may be considered. Noting that $f^*(s)$ does not have a pole at $s = 1$ because that point lies in its ROC, we have

$$\begin{aligned} C &\sim \lim_{s\to 1} \frac{d}{ds}\left((s-1)^2 f^*(s)\frac{\Gamma(2-s)\Gamma(s-1)}{s-1}\right) \\ &= \lim_{s\to 1}\frac{d}{ds}\left(f^*(s)\Gamma(2-s)\Gamma(s)\right). \end{aligned} \tag{19}$$

Since $(d/ds)\Gamma(s) = \Gamma(s)\psi(s)$, where $\psi(x) = (d/dx)\ln\Gamma(x)$ is the digamma function [24, Eq. (8.360)] and substituting from (5), the following result for the asymptotic capacity is obtained:

$$\begin{aligned} C \sim &-\ln(\lambda) + \lim_{s\to 1} \\ &\times\left[\sum_{j=1}^{m} B_j\psi(b_j+B_j s) - \sum_{j=1}^{n} A_j\psi(1-a_j-A_j s)\right. \\ &\left. - \sum_{j=n+1}^{p} A_j\psi(a_j+A_j s) + \sum_{j=m+1}^{q} B_j\psi(1-b_j-B_j s)\right]. \end{aligned} \tag{20}$$

D. Special Cases

As mentioned earlier, the Fox's H-function fading distribution generalizes many well-known recent fading distributions such as the $\alpha{-}\mu$ and the EGK distributions. It is interesting to see how the general expressions derived for the SER and the channel capacity simplify when selecting special parameters corresponding to those distributions.

1) $\alpha{-}\mu$ Distribution: As shown in [19, Tab. V], the $\alpha{-}\mu$ (generalized Gamma) distribution is a special case of the H-function fading distribution for which the parameters are chosen as follows.[2] $\kappa = \beta/\Gamma(\mu)\bar{\gamma}$, and $\lambda = \beta/\bar{\gamma}$ where $\beta = (\Gamma(\mu + 1/\alpha)/\Gamma(\mu))$, $m = q = 1$, $n = p = 0$, $b_1 = \mu - (1/\alpha)$, and $B_1 = 1/\alpha$. Hence, the function $f^*(s)$ has poles only at the points $s = -(b_1 + r)/B_1 = 1 - (\mu + r)\alpha$, $r = 0, 1, \ldots$. As a consequence, $l = 1 - \alpha\mu$, $u \to \infty$, and the ROC of $f^*(s)$ is simply $\Re\{s\} > 1 - \alpha\mu$, which includes the point $s = 1$ as long as $\mu > 0$ and $\alpha > 0$, which is always achieved as required by the definition of the distribution. Thus, the SER is obtained using (7) with $1 - \alpha\mu < \sigma < 1$. Substituting with the aforementioned values into the expressions in Table II, it is straightforward to obtain the exact same results as those previously published in our work [15, Tab III] for $\alpha{-}\mu$ fading, which confirms the versatility of Fox's H-function fading model.

The asymptotic expansions of the basic functions $\mathcal{I}_r(\theta)$, $r = 0, 1, 2$, are obtained either by evaluating the residue of the integrand in (7) at the pole $s = -b_1/B_1 = 1 - \alpha\mu$ or by employing Theorem 2 directly. We should note that, since we have only one simple pole, we have $m' = m = 1$, $N_1 = 1$, and $K_1 = \{1\}$; hence, $E_1 = 1/B_1 = \alpha$. Substituting the $\alpha - \mu$ parameters into (14) will yield the following simplified expressions:

$$\mathcal{I}_0(\mathrm{b}) \sim \frac{\Gamma(1+\alpha\mu)}{\Gamma(1+\mu)}\left(\frac{\beta}{\mathrm{b}\bar{\gamma}}\right)^{\alpha\mu} \tag{21a}$$

$$\mathcal{I}_1(\mathrm{b}) \sim \frac{\Gamma\left(\frac{1}{2}+\alpha\mu\right)}{\sqrt{\mathrm{b}}\,\Gamma(1+\mu)}\left(\frac{\beta}{\mathrm{b}\bar{\gamma}}\right)^{\alpha\mu} \tag{21b}$$

$$\mathcal{I}_2(\mathrm{a},\mathrm{b}) \sim \frac{\sqrt{\mathrm{a}}\,\Gamma(1+\alpha\mu)}{\mathrm{b}\sqrt{2\pi}\,\Gamma(1+\mu)}\,{}_2F_1\left(\frac{1}{2}, 1+\alpha\mu; \frac{3}{2}; -\frac{\mathrm{a}}{2\mathrm{b}}\right)\left(\frac{\beta}{\mathrm{b}\bar{\gamma}}\right)^{\alpha\mu} \tag{21c}$$

which are identical to [15, Eqs. (15) and (17)] with the single exception of a missing b in the denominator of $\mathcal{I}_0(\mathrm{b})$ due to the fact that, in this paper, we are working directly with the conditional SER, $P(\text{error}|\gamma)$ rather than its derivative. Nonetheless, we stress that upon substituting (21) into the expressions in [15, Tab. III], we obtain the exact same expansions obtained in [15, Tab. V].

The exact expression for the channel capacity is obtained either by using (16) with $1 < \sigma < 2$ or by substituting in (18) with the corresponding parameters of the $\alpha{-}\mu$ distribution. This results in the following exact expression for the average channel capacity:

$$C = \frac{1}{\Gamma(\mu)} H^{3,1}_{2,3}\left(\frac{\beta}{\bar{\gamma}} \middle| \begin{array}{c} (0,1),(1,1) \\ (0,1),(0,1),\left(\mu,\frac{1}{\alpha}\right) \end{array}\right). \tag{22}$$

The asymptotic expansion for the channel capacity can also be obtained by substituting into (20) using the special parameters corresponding to the $\alpha{-}\mu$ distribution yielding

$$C \sim \ln(\bar{\gamma}) - \ln(\beta) + \frac{1}{\alpha}\psi(\mu) \tag{23}$$

which is identical to the result reported in [26, Eq. (18)].

[2] In [15], we defined $\bar{\gamma} = (E\{\gamma^\alpha\})^{1/\alpha}$. Here and in [19], $\bar{\gamma}$ is defined as $\bar{\gamma} = E\{\gamma\}$. The final results in both cases are also exactly the same.

TABLE IV
FINAL FORM OF THE P_e FOR THE DIFFERENT MODULATION SCHEMES WITH EGK FADING

Modulation Scheme	P_e
CBFSK	$\frac{1}{2\sqrt{\pi}\Gamma(\mu_s)\Gamma(\mu)} H_{2,3}^{2,2}\left(\frac{2\beta_s\beta}{\bar{\gamma}} \,\middle\vert\, \begin{matrix} (1,1),(\frac{1}{2},1) \\ (\mu_s,\frac{1}{\xi_s}),(\mu,\frac{1}{\xi}),(0,1) \end{matrix} \right)$
M-ary ASK	$\frac{(M-1)}{M\sqrt{\pi}\Gamma(\mu_s)\Gamma(\mu)} H_{2,3}^{2,2}\left(\frac{(M^2-1)\beta_s\beta}{3\bar{\gamma}} \,\middle\vert\, \begin{matrix} (1,1),(\frac{1}{2},1) \\ (\mu_s,\frac{1}{\xi_s}),(\mu,\frac{1}{\xi}),(0,1) \end{matrix} \right)$
M-ary PSK	$\frac{1}{2\sqrt{\pi}\Gamma(\mu_s)\Gamma(\mu)} \left[H_{2,3}^{2,2}\left(\frac{\beta_s\beta}{\bar{\gamma}\sin^2(\frac{\pi}{M})} \,\middle\vert\, \begin{matrix} (1,1),(\frac{1}{2},1) \\ (\mu_s,\frac{1}{\xi_s}),(\mu,\frac{1}{\xi}),(0,1) \end{matrix} \right) \right.$ $\left. + \frac{1}{\sqrt{\pi}} H_{1,0;1,2;1,3}^{0,1;1,1;2,1}\left(\cot^2(\tfrac{\pi}{M}), \frac{\beta_s\beta}{\bar{\gamma}\sin^2(\frac{\pi}{M})} \,\middle\vert\, \begin{matrix} (\frac{1}{2};1,1) & (1,1) & (1,1) \\ - & (\frac{1}{2},1),(0,1) & (\mu_s,\frac{1}{\xi_s}),(\mu,\frac{1}{\xi}),(0,1) \end{matrix} \right) \right]$
M-QAM	$\frac{2(\sqrt{M}-1)}{M\sqrt{\pi}\Gamma(\mu_s)\Gamma(\mu)} \left[H_{2,3}^{2,2}\left(\frac{2(M-1)\beta_s\beta}{3\bar{\gamma}} \,\middle\vert\, \begin{matrix} (1,1),(\frac{1}{2},1) \\ (\mu_s,\frac{1}{\xi_s}),(\mu,\frac{1}{\xi}),(0,1) \end{matrix} \right) \right.$ $\left. + \frac{\sqrt{M}-1}{\sqrt{\pi}} H_{1,0;1,2;1,3}^{0,1;1,1;2,1}\left(1, \frac{2(M-1)\beta_s\beta}{3\bar{\gamma}} \,\middle\vert\, \begin{matrix} (\frac{1}{2};1,1) & (1,1) & (1,1) \\ - & (\frac{1}{2},1),(0,1) & (\mu_s,\frac{1}{\xi_s}),(\mu,\frac{1}{\xi}),(0,1) \end{matrix} \right) \right]$
DBPSK	$\frac{1}{2\Gamma(\mu_s)\Gamma(\mu)} H_{1,2}^{2,1}\left(\frac{\beta_s\beta}{\bar{\gamma}} \,\middle\vert\, \begin{matrix} (1,1) \\ (\mu_s,\frac{1}{\xi_s}),(\mu,\frac{1}{\xi}) \end{matrix} \right)$
NC M-ary FSK	$\frac{1}{\Gamma(\mu_s)\Gamma(\mu)} \sum_{n=1}^{M-1} (-1)^{n+1} \binom{M-1}{n} \frac{n}{n+1} H_{1,2}^{2,1}\left(\frac{(n+1)\beta_s\beta}{n\bar{\gamma}} \,\middle\vert\, \begin{matrix} (1,1) \\ (\mu_s,\frac{1}{\xi_s}),(\mu,\frac{1}{\xi}) \end{matrix} \right)$

TABLE V
ASYMPTOTIC EXPRESSIONS FOR P_e FOR THE DIFFERENT MODULATION SCHEMES OVER EGK FADING. $\mu_1 = \mu_s$, $\mu_2 = \mu$, $\xi_1 = \xi_s$, AND $\xi_2 = \xi$, $j = 1, 2$. THE VALUES OF m', E_j, N_j ARE AS DISCUSSED IN SECTION II-D2

Modulation Scheme	Asymptotic P_e
CBFSK	$\frac{1}{2\sqrt{\pi}} \sum_{j=1}^{m'} \frac{E_j \Gamma\left(\frac{1}{2}+\mu_j\xi_j\right)}{\xi_j \Gamma(\mu_{3-j})\Gamma(1+\mu_j)} \left[\ln\left(\frac{\bar{\gamma}}{2\beta_s\beta} \right) \right]^{N_j-1} \left(\frac{2\beta_s\beta}{\bar{\gamma}} \right)^{\mu_j\xi_j}$
M-ary ASK	$\frac{M-1}{M\sqrt{\pi}} \sum_{j=1}^{m'} \frac{E_j \Gamma\left(\frac{1}{2}+\mu_j\xi_j\right)}{\xi_j \Gamma(\mu_{3-j})\Gamma(1+\mu_j)} \left[\ln\left(\frac{3\bar{\gamma}}{(M^2-1)\beta_s\beta} \right) \right]^{N_j-1} \left(\frac{(M^2-1)\beta_s\beta}{3\bar{\gamma}} \right)^{\mu_j\xi_j}$
M-ary PSK	$\frac{1}{\sqrt{\pi}} \sum_{j=1}^{m'} \left\{ \frac{E_j}{\xi_j \Gamma(\mu_{3-j})\Gamma(1+\mu_j)} \left[\ln\left(\frac{\sin^2\left(\frac{\pi}{M}\right)\bar{\gamma}}{\beta_s\beta} \right) \right]^{N_j-1} \left(\frac{\beta_s\beta}{\sin^2\left(\frac{\pi}{M}\right)\bar{\gamma}} \right)^{\mu_j\xi_j} \right.$ $\left. \times \left[\frac{1}{2}\Gamma\left(\frac{1}{2}+\mu_j\xi_j\right) + \frac{\cot(\pi/M)}{\sqrt{\pi}} {}_2F_1\left(\frac{1}{2}, 1+\mu_j\xi_j; \frac{3}{2}; -\cot^2\left(\frac{\pi}{M}\right) \right) \right] \right\}$
M-QAM	$\frac{2(\sqrt{M}-1)/\sqrt{M}}{\sqrt{\pi}} \sum_{j=1}^{m'} \left\{ \frac{E_j}{\xi_j \Gamma(\mu_{3-j})\Gamma(1+\mu_j)} \left[\ln\left(\frac{3\bar{\gamma}}{2(M-1)\beta_s\beta} \right) \right]^{N_j-1} \left(\frac{2(M-1)\beta_s\beta}{3\bar{\gamma}} \right)^{\mu_j\xi_j} \right.$ $\left. \times \left[\frac{1}{\sqrt{M}}\Gamma\left(\frac{1}{2}+\mu_j\xi_j\right) + 2\frac{\sqrt{M}-1}{\sqrt{M\pi}} {}_2F_1\left(\frac{1}{2}, 1+\mu_j\xi_j; \frac{3}{2}; -1 \right) \right] \right\}$
DBPSK	$\frac{1}{2} \sum_{j=1}^{m'} \frac{E_j \Gamma(1+\mu_j\xi_j)}{\xi_j \Gamma(\mu_{3-j})\Gamma(1+\mu_j)} \left[\ln\left(\frac{\bar{\gamma}}{\beta_s\beta} \right) \right]^{N_j-1} \left(\frac{\beta_s\beta}{\bar{\gamma}} \right)^{\mu_j\xi_j}$
NC M-ary FSK	$\sum_{n=1}^{M-1} (-1)^{n+1} \binom{M-1}{n} \frac{1}{(n+1)} \sum_{j=1}^{m'} \frac{E_j \Gamma(1+\mu_j\xi_j)}{\xi_j \Gamma(\mu_{3-j})\Gamma(1+\mu_j)} \left[\ln\left(\frac{n\bar{\gamma}}{(n+1)\beta_s\beta} \right) \right]^{N_j-1} \left(\frac{(n+1)\beta_s\beta}{n\bar{\gamma}} \right)^{\mu_j\xi_j}$

2) EGK Distribution: The second special case considered here is that of the EGK distribution. According to [19, Tab. V], this distribution can be obtained from Fox's H-function fading distribution by setting the parameters of the latter as follows: $\kappa = (\beta_s\beta/\Gamma(\mu_s)\Gamma(\mu)\bar{\gamma})$, and $\lambda = \beta_s\beta/\bar{\gamma}$, where $\bar{\gamma} = E\gamma$, $\beta_s = (\Gamma(\mu_s + (1/\xi_s))/\Gamma(\mu_s))$, and $\beta = (\Gamma(\mu + (1/\xi))/\Gamma(\mu))$, $m = q = 2$, $n = p = 0$, $b_1 = \mu_s - \xi_s^{-1}$, $B_1 = \xi_s^{-1}$, $b_2 = \mu - \xi^{-1}$, and $B_2 = \xi^{-1}$. Hence, the function $f^*(s)$ in this case has two sets of poles: at $s = -(b_1 + r_1)/B_1 = 1 - (\mu_s + r_1)\xi_s$ and at $s = -(b_2 + r_2)/B_2 = 1 - (\mu + r_2)\xi$ where r_1 and r_2 are nonnegative integers. Therefore, we have $l = 1 - \min(\mu_s\xi_s, \mu\xi)$, $u \to \infty$, and the ROC for $f^*(s)$ is $\Re\{s\} > 1 - \min(\mu_s\xi_s, \mu\xi)$. Since we have $\mu_s > 0.5$, $\xi_s > 0$, $\mu > 0.5$, and $\xi > 0$, as dictated by the distribution definition, we always guarantee that the ROC includes the point $s = 1$. Substituting with the aforementioned values of the EGK fading model into the generalized expressions of SER in Table II, it is straightforward to obtain the exact SER expression of different modulation schemes under EGK channel fading as summarized in Table IV. It is important to note here that these SER expressions for the EGK model are novel and have never been reported before in the literature.

Unlike the case of $\alpha-\mu$ distribution, we have $m = 2$; hence, the asymptotic expansion of the SER is derived by computing the residues at two poles: $s_1 = -b_1/B_1 = 1 - \mu_s\xi_s$, and $s_2 = -b_2/B_2 = 1 - \mu\xi$. In fact, we have three possible scenarios. First, the two poles are simple, which happens when both $\mu_s - \mu\xi/\xi_s$, and $\mu - \mu_s\xi_s/\xi$ are neither a negative integer nor zero. In that case, we have $m' = 2$, $N_1 = N_2 = 1$, $K_1 = \{1\}$, $K_2 = \{2\}$, $E_1 = \xi_s\Gamma(\mu - \mu_s\xi_s/\xi)$, and $E_2 = \xi\Gamma(\mu_s - \mu\xi/\xi_s)$. Second, the two poles coincide, which happens when $\mu_s\xi_s = \mu\xi$. In that case, $m' = 1$,$N_1 = 2$, $K_1 = \{1, 2\}$, and $E_1 = \xi\xi_s$. Finally, one of the poles is simple, whereas the other coincides with a third pole, which happens when either $\mu_s - \mu\xi/\xi_s$ or $\mu - \mu_s\xi_s/\xi$ is a negative integer. If $\mu - \mu_s\xi_s/\xi = -r$ where r is a positive integer, it can be shown that $m' = 2$, $N_1 = 2$, $K_1 = \{1, 2\}$, $E_1 = (-1)^r\xi\xi_s/r!$, $N_2 = 1$, $K_2 = \{2\}$, and $E_2 = \xi\Gamma(\mu_s - \mu\xi/\xi_s)$. If $\mu_s - \mu\xi/\xi_s = -r$ where r is a positive integer, then $m' = 2$, $N_1 = 1$, $K_1 = \{1\}$, $E_1 = \xi_s\Gamma(\mu - \mu_s\xi_s/\xi)$, $N_2 = 2$, $K_2 = \{1, 2\}$, and $E_2 = (-1)^r\xi\xi_s/r!$. Substituting the EGK parameters into (14) while taking into consideration the previous scenarios, we obtain the expressions shown in (24), for the basic functions $\mathcal{I}_r(\theta)$. In these expressions, we define, for convenience, $\mu_1 = \mu_s$, $\mu_2 = \mu$, $\xi_1 = \xi_s$, and $\xi_2 = \xi$, $j = 1, 2$. Substituting (24) into the expressions in [15, Tab. III], the asymptotic expansions of the SERs for different modulation schemes are obtained as in Table V

$$\mathcal{I}_0(\mathrm{b}) \sim \sum_{j=1}^{m'} \frac{E_j\Gamma\left(1+\mu_j\xi_j\right)}{\xi_j\Gamma\left(\mu_{3-j}\right)\Gamma\left(1+\mu_j\right)} \times \left[\ln\left(\frac{\mathrm{b}\bar{\gamma}}{\beta_s\beta}\right)\right]^{N_j-1}\left(\frac{\beta_s\beta}{\mathrm{b}\bar{\gamma}}\right)^{\mu_j\xi_j} \tag{24a}$$

$$\mathcal{I}_1(\mathrm{b}) \sim \frac{1}{\sqrt{\mathrm{b}}}\sum_{j=1}^{m'} \frac{E_j\Gamma\left(\frac{1}{2}+\mu_j\xi_j\right)}{\xi_j\Gamma\left(\mu_{3-j}\right)\Gamma\left(1+\mu_j\right)} \times \left[\ln\left(\frac{\mathrm{b}\bar{\gamma}}{\beta_s\beta}\right)\right]^{N_j-1}\left(\frac{\beta_s\beta}{\mathrm{b}\bar{\gamma}}\right)^{\mu_j\xi_j} \tag{24b}$$

$$\mathcal{I}_2(\mathrm{a},\mathrm{b}) \sim \frac{\sqrt{\mathrm{a}}}{\mathrm{b}\sqrt{2\pi}}\sum_{j=1}^{m'} \frac{E_j\Gamma\left(1+\mu_j\xi_j\right)}{\xi_j\Gamma\left(\mu_{3-j}\right)\Gamma\left(1+\mu_j\right)} \times {}_2F_1\left(\frac{1}{2}, 1+\mu_j\xi_j; \frac{3}{2}; -\frac{\mathrm{a}}{2\mathrm{b}}\right) \times \left[\ln\left(\frac{\mathrm{b}\bar{\gamma}}{\beta_s\beta}\right)\right]^{N_j-1}\left(\frac{\beta_s\beta}{\mathrm{b}\bar{\gamma}}\right)^{\mu_j\xi_j}. \tag{24c}$$

The channel capacity may also be driven through the use of (18) after substituting with the parameters of the EGK distribution. This easily yields the following expression for the channel capacity:

$$C = \frac{1}{\Gamma(\mu_s)\Gamma(\mu)} H_{2,4}^{4,1}\left(\frac{\beta_s\beta}{\bar{\gamma}}\middle| \begin{matrix} (0,1),(1,1) \\ (0,1),(0,1),\left(\mu_s,\frac{1}{\xi_s}\right),\left(\mu,\frac{1}{\xi}\right) \end{matrix}\right) \tag{25}$$

which, after some straightforward manipulations, can reduce to [5, Eq. (15)]. The asymptotic expansion is also obtained by either taking the residue of the integrand in (16) at the double pole $s = 1$ or substituting the EGK parameters in (20). After some simplifications, we reach the following asymptotic expansion of the channel capacity for EGK fading:

$$C \sim \ln(\bar{\gamma}) - \ln(\beta_s\beta) + \frac{1}{\xi_s}\psi(\mu_s) + \frac{1}{\xi}\psi(\mu). \tag{26}$$

III. Multiple-Branch Communications

Here, we consider deriving the exact and asymptotic SER expressions for various diversity combiners assuming statistically independent but not necessarily identical branches.

A. System Model

Suppose we have an L-branch receiver, each of which has an instantaneous SNR γ_l, $l = 1, \ldots, L$ with a pdf

$$f_{\gamma_l}(\gamma_l) = \kappa_l H_{p_l,q_l}^{m_l,n_l}\left(\lambda_l\gamma_l\middle| \begin{matrix} \left(a_j^{(l)}, A_j^{(l)}\right)_{j=1:p_l} \\ \left(b_j^{(l)}, B_j^{(l)}\right)_{j=1:q_l} \end{matrix}\right), \quad \gamma_l > 0. \tag{27}$$

Obviously, the existence and convergence conditions will be similar to the case of single-branch communications. The only difference will be in adding the subscript l wherever appropriate. In our analysis, we will make use of the definition of the multivariate H-function in (28), shown at the bottom of the page [27]. For convenience, we shall adopt the abbreviated notation for the multivariate-H function in (29) and (30), shown at the bottom of the next page, where the square brackets indicate replication across different dimensions.

$$H_{p,q:p_1,q_1,\ldots,p_L,q_L}^{0,n:m_1,n_1,\ldots,m_L,n_L}\left(\begin{matrix}\zeta_1\\ \vdots \\ \zeta_L\end{matrix}\middle| \begin{matrix} \left(c_j : C_j^{(1)},\ldots,C_j^{(L)}\right)_{j=1:p} & \left(a_j^{(1)}, A_j^{(1)}\right)_{j=1:p_1} & \cdots & \left(a_j^{(L)}, A_j^{(L)}\right)_{j=1:p_L} \\ \left(d_j : D_j^{(1)},\ldots,D_j^{(L)}\right)_{j=1:q} & \left(b_j^{(1)}, B_j^{(1)}\right)_{j=1:q_1} & \cdots & \left(b_j^{(L)}, B_j^{(L)}\right)_{j=1:q_L} \end{matrix}\right)$$

$$= \frac{1}{(2\pi i)^L}\int_{\mathcal{L}_1}\cdots\int_{\mathcal{L}_L} \Xi\left(s_1,\ldots,s_L\right)\prod_{l=1}^{L}\left(\phi_l\left(s_l\right)\zeta_l^{-s_l}\right) ds_1,\ldots,ds_L \tag{28}$$

B. Symbol-Error-Rate Analysis

The output of a wide range of diversity receivers can be generally written in the following form [28][3]:

$$\gamma_c = \eta_0 \left(\sum_{l=1}^{L} \gamma_l^{\eta_1} \right)^{\frac{1}{\eta_1}} \tag{31}$$

where $\{\eta_0, \eta_1\} = \{1, 1\}$ for MRC, and $\{\eta_0, \eta_1\} = \{1/L, 1/2\}$ for EGC. For SC, it is well known that $\gamma_c = \max_{l=1,\ldots,L} \gamma_l$, which corresponds to $\eta_0 = 1$ and $\eta_1 \to \infty$. The unconditional SER is given by

$$P_e = \int_{\boldsymbol{\gamma}} f_{\boldsymbol{\gamma}}(\boldsymbol{\gamma}) h(\gamma_c)\, d\boldsymbol{\gamma} \tag{32}$$

where $\int_{\boldsymbol{\gamma}}$ is a shorthand for $\int_{\gamma_1=0}^{\infty}, \ldots, \int_{\gamma_L=0}^{\infty}$, $f_{\boldsymbol{\gamma}}(\boldsymbol{\gamma})$ is the joint pdf of $\boldsymbol{\gamma} = [\gamma_1, \ldots, \gamma_L]$, and $h(\gamma_c)$ is the conditional SER, which can be considered a function of $\boldsymbol{\gamma}$ after substituting from (31) for γ_c. We have provided a generalization of Theorem 1 to the case of L-branch diversity receivers in [15, Th. 2], which is reproduced here for convenience.

Theorem 3: Consider an L-branch diversity receiver in which the fading channels are independent, and the joint pdf of the SNRs at each branch is $f_{\boldsymbol{\gamma}}(\boldsymbol{\gamma})$. Suppose that the Mellin transforms of $f_{\boldsymbol{\gamma}}(\boldsymbol{\gamma})$ and $h(\gamma_c)$ are $f^*(\mathbf{s})$ and $h^*(\mathbf{s})$, respectively. The SER at the combiner output is given by the relation

$$P_e = \frac{1}{(2\pi i)^L} \int_{\mathbf{s}} f^*(\mathbf{s}) h^*(1 - \mathbf{s}) d\mathbf{s} \tag{33}$$

where $\mathbf{s} = [s_1, \ldots, s_L]^{\mathrm{T}}$, 1 is the $L \times 1$ all-ones vector, and $\int_{\mathbf{s}}$ is a shorthand for $\int_{s_1=\sigma_1-i\infty}^{\sigma_1+i\infty} \cdots \int_{s_L=\sigma_L-i\infty}^{\sigma_L+i\infty}$. The constants σ_l, $l = 1, \ldots, L$ are chosen such that the vector $\boldsymbol{\sigma} = [\sigma_1, \ldots, \sigma_L]$ lies in the region of definitions of $f^*(\mathbf{s})$ and $h^*(1 - \mathbf{s})$.

To evaluate the SER integral in (33), both $f^*(\mathbf{s})$ and $h^*(\mathbf{s})$ are needed. The former can be easily obtained from $f^*(\mathbf{s}) = \prod_{l=1}^{L} f^*(s_l)$ due to the independence assumption. As for the latter, because of the very special form of γ_c, we are able to derive an interesting relation for the L-dimensional Mellin transform of $h(\gamma_c)$, as shown in the following theorem.

Theorem 4: If γ_c is given by (31), then the L-dimensional Mellin transform of $h(\gamma_c)$ is given by

$$h^*(\mathbf{s}) = \frac{\eta_0^{-\sum_{l=1}^{L} s_l} \prod_{l=1}^{L} \Gamma(s_l/\eta_1)}{\eta_1^{L-1} \Gamma\left(\frac{1}{\eta_1} \sum_{l=1}^{L} s_l\right)} \int_{\gamma_c=0}^{\infty} h(\gamma_c)\, \gamma_c^{\sum_{l=1}^{L} s_l - 1}\, d\gamma_c. \tag{34}$$

Moreover, if $h(\gamma_c) = \int_{u=\gamma_c}^{\infty} g(u) du$, then

$$h^*(\mathbf{s}) = \frac{\prod_{l=1}^{L} \Gamma(s_l/\eta_1)}{\eta_1^{L-1} \Gamma\left(\frac{1}{\eta_1} \sum_{l=1}^{L} s_l\right) \sum_{l=1}^{L} s_l} \int_{u=0}^{\infty} g(u) u^{\sum_{l=1}^{L} s_l} du. \tag{35}$$

Proof: The Mellin transform of $h(\gamma_c)$ is given by

$$h^*(\mathbf{s}) = \int_{\gamma_1=0}^{\infty} \cdots \int_{\gamma_L=0}^{\infty} h\left(\eta_0 \left(\sum_{l=1}^{L} \gamma_l^{\eta_1} \right)^{\frac{1}{\eta_1}} \right) \times \prod_{l=1}^{L} \gamma_l^{s_l - 1} d\gamma_L, \ldots, d\gamma_1. \tag{36}$$

Performing the change of variables $v_l = \sum_{k=1}^{l} \gamma_k^{\eta_1}$ and noting that the Jacobian of the transformation is $|J| = \eta_1{}^{-L} v_1^{1/\eta_1 - 1} \prod_{l=2}^{L} (v_l - v_{l-1})^{1/\eta_1 - 1}$, we easily obtain the following expression for $h^*(\mathbf{s})$:

$$h^*(\mathbf{s}) = \frac{1}{\eta_1^L} \int_{v_L=0}^{\infty} h\left(\eta_0 v_L^{\frac{1}{\eta_1}} \right) \times \left(\int_{v_{L-1}=0}^{v_L} \cdots \int_{v_1=0}^{v_2} v_1^{\frac{s_1}{\eta_1} - 1} \prod_{l=2}^{L} (v_l - v_{l-1})^{\frac{s_l}{\eta_1} - 1} dv_1 \ldots, dv_{L-1} \right) dv_L. \tag{37}$$

[3]In fact, the relation presented in [28] takes the form $\gamma_c = \eta((1/L) \sum_{l=1}^{L} \gamma_l^p)^q$, where p and q are not to be confused with the definition of p and q in this paper. Nonetheless, in almost all diversity schemes of interest (even in [28] itself), we have $q = 1/p$. Hence, by setting $\eta_0 = \eta L^{-1/p}$ and $q = 1/p$, we get the relation in (31).

$$\Xi(s_1, \ldots, s_L) = \frac{\prod_{j=1}^{n} \Gamma\left(1 - c_j - \sum_{l=1}^{L} C_j^{(l)} s_l\right)}{\prod_{j=n+1}^{p} \Gamma\left(c_j + \sum_{l=1}^{L} C_j^{(l)} s_l\right) \prod_{j=1}^{q} \Gamma\left(1 - d_j - \sum_{l=1}^{L} D_j^{(l)} s_l\right)} \tag{29a}$$

$$\phi_l(s_l) = \frac{\prod_{j=1}^{m_l} \Gamma\left(b_j^{(l)} + B_j^{(l)} s_l\right) \prod_{j=1}^{n_l} \Gamma\left(1 - a_j^{(l)} - A_j^{(l)} s_l\right)}{\prod_{j=n_l+1}^{p_l} \Gamma\left(a_j^{(l)} + A_j^{(l)} s_l\right) \prod_{j=m_l+1}^{q_l} \Gamma\left(1 - b_j^{(l)} - B_j^{(l)} s_l\right)}, \qquad l = 1, \ldots, L. \tag{29b}$$

$$H_{p,q:[p_l,q_l]_{l=1:L}}^{0,n:[m_l,n_l]_{l=1:L}} \left(\begin{array}{c} \zeta_1 \\ \vdots \\ \zeta_L \end{array} \middle| \begin{array}{c} \left(c_j : \left\{C_j^{(l)}\right\}_{l=1:L}\right)_{j=1:p} \\ \left(d_j : \left\{D_j^{(l)}\right\}_{l=1:L}\right)_{j=1:q} \end{array} \begin{bmatrix} \left(a_j^{(l)}, A_j^{(l)}\right)_{j=1:p_l} \\ \left(b_j^{(l)}, B_j^{(l)}\right)_{j=1:q_l} \end{bmatrix}_{l=1:L} \right) \tag{30}$$

TABLE VI
BASIC COMPONENTS OF $h(\gamma_c)$ TOGETHER WITH THEIR MELLIN TRANSFORMS

$h_{cr}(\gamma;\theta)$	Mellin transform
$h_{c0}(\gamma_c;\mathrm{b}) = e^{-\mathrm{b}\gamma_c}$	$h_0^*(\mathbf{s};\mathrm{b}) = \frac{\eta_0^{-\sum_{l=1}^L s_l}}{\eta_1{}^{L-1}} \frac{\Gamma\left(\sum_{l=1}^L s_l\right)\prod_{l=1}^L \mathrm{b}^{-s_l}\Gamma(s_l/\eta_1)}{\Gamma\left(\frac{1}{\eta_1}\sum_{l=1}^L s_l\right)}$
$h_{c1}(\gamma_c;\mathrm{b}) = \int_{u=\gamma_c}^{\infty} u^{-1/2}e^{-\mathrm{b}u}du$	$h_1^*(\mathbf{s};\mathrm{b}) = \frac{\eta_0^{-\sum_{l=1}^L s_l}}{\eta_1{}^L\sqrt{\mathrm{b}}} \frac{\Gamma\left(\frac{1}{2}+\sum_{l=1}^L s_l\right)\prod_{l=1}^L \mathrm{b}^{-s_l}\Gamma(s_l/\eta_1)}{\Gamma\left(1+\frac{1}{\eta_1}\sum_{l=1}^L s_l\right)}$
$h_{c2}(\gamma_c;\mathrm{a},\mathrm{b}) = \int_{u=\gamma_c}^{\infty} u^{-1/2}e^{-\mathrm{b}u}Q'(\sqrt{\mathrm{a}u})du$	$h_2^*(\mathbf{s};\mathrm{a},\mathrm{b}) = \frac{\eta_0^{-\sum_{l=1}^L s_l}}{2\eta_1{}^L\sqrt{\mathrm{b}\pi}} \frac{\prod_{l=1}^L \mathrm{b}^{-s_l}\Gamma(s_l/\eta_1)}{\Gamma\left(1+\frac{1}{\eta_1}\sum_{l=1}^L s_l\right)} \times \frac{1}{2\pi i}\int_{w=c_2-i\infty}^{c_2+i\infty} \frac{\Gamma(\frac{1}{2}-w)}{w}\Gamma\left(w+\frac{1}{2}+\sum_{l=1}^L s_l\right)\left(\frac{\mathrm{a}}{2\mathrm{b}}\right)^w dw$

The integration between parenthesis in (37) is simply evaluated using the definition of the beta function [24, Eq. (8.380.1)] with proper changes of variables and is equal to $(\prod_{l=1}^L \Gamma(s_l/\eta_1)/\Gamma(\sum_{l=1}^L s_l/\eta_1))v_L^{1/\eta_1\sum_{l=1}^L s_l - 1}$. Hence, we have

$$h^*(\mathbf{s}) = \frac{\prod_{l=1}^{L}\Gamma\left(\frac{s_l}{\eta_1}\right)}{\eta_1^L\Gamma\left(\sum_{l=1}^{L} s_l/\eta_1\right)} \int_{v_L=0}^{\infty} h\left(\eta_0 v_L^{\frac{1}{\eta_1}}\right) v_L^{\frac{1}{\eta_1}\sum_{l=1}^{L} s_l - 1} dv_L. \tag{38}$$

Performing the change of variable $\gamma_c = \eta_0 v_L^{1/\eta_1}$, the result in (34) follows. Equation (35) follows from (34) by substituting $h(\gamma_c) = \int_{u=\gamma_c}^{\infty} g(u)du$ into it and changing the order of the resultant double integration. This concludes the proof of the theorem. □

It is worth noting that, for SC, the limit as $\eta_0 = 1$, $\eta_1 \to \infty$ exists, and is given by the following corollary.

Corollary 1: As $\eta_0 = 1$, $\eta_1 \to \infty$, we have

$$\begin{aligned} h^*(\mathbf{s}) &= \frac{\sum_{l=1}^{L} s_l}{\prod_{l=1}^{L} s_l} \int_{\gamma_c=0}^{\infty} h\left(\gamma_c\right)\gamma_c^{\sum_{l=1}^{L} s_l - 1} d\gamma_c \\ &= \frac{1}{\prod_{l=1}^{L} s_l} \int_{u=0}^{\infty} g(u) u^{\sum_{l=1}^{L} s_l} du. \end{aligned} \tag{39}$$

1) Exact Expressions: Similar to the case of single-branch communications, $h(\gamma_c)$ contains one or more of the terms shown in the first column of Table VI. It can also be shown that the region of definition of $h^*(\mathbf{s})$ is always given by $\Omega_h = \{\mathbf{s} : s_1 > 0, \ldots, s_L > 0\}$. Hence, the region of definition of $h^*(1-\mathbf{s})$ is $\Omega'_h = \{\mathbf{s} : s_1 < 1, \ldots, s_L < 1\}$. Furthermore, as mentioned earlier, since $f_{\boldsymbol{\gamma}}(\boldsymbol{\gamma})$ is a pdf, it is always guaranteed that the vector $1 \in \Omega$, where Ω is the region of definition of $f^*(\mathbf{s})$. Thus, it is also guaranteed that the intersection between the two regions Ω and Ω'_h is not empty since the vector 1 belongs to both Ω and the closure of Ω'_h. Moreover, the vector $\boldsymbol{\sigma}$ must belong to this intersection for the validity of Theorem 3. Similar to the case of single-branch communications, the function $h(\gamma_c)$ is usually given as a linear combination of one or more of the functions $h_{cr}(\gamma;\theta)$, $r = 0, 1, 2$, listed in Table VI. Therefore, the exact SER is a linear combination of the basic functions defined by

$$\mathcal{I}_{cr}(\theta) \equiv \frac{1}{(2\pi i)^L}\int_{\mathbf{s}} f^*(\mathbf{s})h_{cr}^*(1-\mathbf{s};\theta)d\mathbf{s}, \quad r = 0, 1 \text{ and } 2 \tag{40}$$

where the functions $h_{cr}^*(\mathbf{z})$ are obtained with the aid of Theorem 4 and are listed in Table VI. Expressions for $\mathcal{I}_{cr}(\theta)$ with different modulation schemes are stated in Table VII. Using these expressions in the corresponding entries in [15, Table III], the expressions of the SER for the different combining and modulation schemes over the Fox's H-function fading channel directly follow. However, they are not presented here due to tight space limitations.

2) Asymptotic Expansions: The asymptotic expansions of the SER for large average SNRs are obtained using the exact same way employed with single-branch communications. In this case, we should compute the residue at the points $\mathbf{s} = (s_1, \ldots, s_L)$, where $s_l \in \{-(b_1^{(l)}/B_1^{(l)}), \ldots, -(b_{m_l}^{(l)}/B_{m_l}^{(l)})\}$, $l = 1, \ldots, L$. However, this will result in a number of terms equal to $\prod_{l=1}^L m_l$. Although it is possible to compute all of them, we found that[4] in most cases, only one dominates the sum, namely, the one corresponding to the pole $\mathbf{s} = (s_1^*, \ldots, s_L^*)$, where $s_l^* = -\min_{j=1,\ldots,m_l}(b_j^{(l)}/B_j^{(l)})$. Therefore, we may further simplify the asymptotic expansions by considering only that pole. Defining $j_l = \arg\max_{j=1,\ldots,m_l}(b_j^{(l)}/B_j^{(l)})$, we get the expressions in (41), for $\mathcal{I}_{cr}(\theta)$, where $K = \prod_{l=1}^L \kappa_l$, $\Lambda = \prod_{l=1}^L \lambda_l$, $N_j^{(l)}$ is the order of the pole $s_j^{(l)} = -b_j^{(l)}/B_j^{(l)}$, and the constants $E_j^{(l)}$ are given in Theorem 2 after adding the superscript $^{(l)}$ whenever appropriate. It can be shown that the ratio K/Λ depends only on the distribution parameters. Therefore, we prefer to represent the above expressions in terms of that ratio. Asymptotic expansions of the basic functions for the three considered diversity combiners are given in Table VIII. Plugging these expressions

[4] We would like to thank one of the reviewers for drawing our attention to this.

TABLE VII
EXACT EXPRESSIONS FOR $\mathcal{I}_{c0}(\mathrm{b})$, $\mathcal{I}_{c1}(\mathrm{b})$, AND $\mathcal{I}_{c2}(\mathrm{a},\mathrm{b})$ FOR DIFFERENT DIVERSITY COMBINING RECEIVERS SUBJECT TO GENERAL FOX'S H-FUNCTION FADING. $K=\prod_{l=1}^{L}\kappa_l$ AND $\Lambda=\prod_{l=1}^{L}\lambda_l$

Diversity	Expressions for $\mathcal{I}_{c0}(\mathrm{b})$, $\mathcal{I}_{c1}(\mathrm{b})$, and $\mathcal{I}_{c2}(\mathrm{a},\mathrm{b})$
MRC	$\mathcal{I}_{c0}(\mathrm{b})=\frac{K}{\Lambda}\prod_{l=1}^{L}H^{m_l,n_l+1}_{p_l+1,q_l}\left(\frac{\lambda_l}{\mathrm{b}}\middle\vert\begin{matrix}(1,1),(a_j^{(l)}+A_j^{(l)},A_j^{(l)})_{j=1:p_l}\\(b_j^{(l)}+B_j^{(l)},B_j^{(l)})_{j=1:q_l}\end{matrix}\right)$
	$\mathcal{I}_{c1}(\mathrm{b})=\frac{K/\Lambda}{\sqrt{\mathrm{b}}}H^{0,1:[m_l,n_l+1]_{l=1:L}}_{1,1:[p_l+1,q_l]_{l=1:L}}\left(\begin{matrix}\lambda_1/\mathrm{b}\\\vdots\\\lambda_L/\mathrm{b}\end{matrix}\middle\vert\begin{matrix}(\frac{1}{2}:\{1\}_{l=1:L})\\(0:\{1\}_{l=1:L})\end{matrix}\quad\left[\begin{matrix}(1,1),(a_j^{(l)}+A_j^{(l)},A_j^{(l)})_{j=1:p_l}\\(b_j^{(l)}+B_j^{(l)},B_j^{(l)})_{j=1:q_l}\end{matrix}\right]_{l=1:L}\right)$
	$\mathcal{I}_{c2}(\mathrm{a},\mathrm{b})=\frac{K/\Lambda}{2\sqrt{\pi\mathrm{b}}}H^{0,1:(1,1),[m_l,n_l+1]_{l=1:L}}_{1,1:(1,2),[p_l+1,q_l]_{l=1:L}}\left(\begin{matrix}\mathrm{a}/2\mathrm{b}\\\lambda_1/\mathrm{b}\\\vdots\\\lambda_L/\mathrm{b}\end{matrix}\middle\vert\begin{matrix}(\frac{1}{2}:1,\{1\}_{l=1:L})\\(0:0,\{1\}_{l=1:L})\end{matrix}\quad\begin{matrix}(1,1)\\(\frac{1}{2},1),(0,1)\end{matrix}\quad\left[\begin{matrix}(1,1),(a_j^{(l)}+A_j^{(l)},A_j^{(l)})_{j=1:p_l}\\(b_j^{(l)}+B_j^{(l)},B_j^{(l)})_{j=1:q_l}\end{matrix}\right]_{l=1:L}\right)$
EGC	$\mathcal{I}_{c0}(\mathrm{b})=\frac{K}{\Lambda}2^L\sqrt{\pi}H^{0,0:[m_l,n_l+1]_{l=1:L}}_{0,1:[p_l+1,q_l]_{l=1:L}}\left(\begin{matrix}\lambda_1L/4\mathrm{b}\\\vdots\\\lambda_LL/4\mathrm{b}\end{matrix}\middle\vert\begin{matrix}-\\(\frac{1}{2},\{1\}_{l=1:L})\end{matrix}\quad\left[\begin{matrix}(1,2),(a_j^{(l)}+A_j^{(l)},A_j^{(l)})_{j=1:p_l}\\(b_j^{(l)}+B_j^{(l)},B_j^{(l)})_{j=1:q_l}\end{matrix}\right]_{l=1:L}\right)$
	$\mathcal{I}_{c1}(\mathrm{b})=\frac{(K/\Lambda)2^L\sqrt{\pi}}{\sqrt{\mathrm{b}}}H^{0,0:[m_l,n_l+1]_{l=1:L}}_{0,1:[p_l+1,q_l]_{l=1:L}}\left(\begin{matrix}\lambda_1L/4\mathrm{b}\\\vdots\\\lambda_LL/4\mathrm{b}\end{matrix}\middle\vert\begin{matrix}-\\(0:\{1\}_{l=1:L})\end{matrix}\quad\left[\begin{matrix}(1,2),(a_j^{(l)}+A_j^{(l)},A_j^{(l)})_{j=1:p_l}\\(b_j^{(l)}+B_j^{(l)},B_j^{(l)})_{j=1:q_l}\end{matrix}\right]_{l=1:L}\right)$
	$\mathcal{I}_{c2}(\mathrm{a},\mathrm{b})=\frac{(K/\Lambda)2^L}{2\sqrt{\mathrm{b}\pi}}H^{0,1:(1,1),[m_l,n_l+1]_{l=1:L}}_{1,1:(1,2),[p_l+1,q_l]_{l=1:L}}\left(\begin{matrix}\mathrm{a}/2\mathrm{b}\\\lambda_1L/\mathrm{b}\\\vdots\\\lambda_LL/\mathrm{b}\end{matrix}\middle\vert\begin{matrix}(\frac{1}{2}:1,\{1\}_{l=1:L})\\(0:0,\{2\}_{l=1:L})\end{matrix}\quad\begin{matrix}(1,1)\\(\frac{1}{2},1),(0,1)\end{matrix}\quad\left[\begin{matrix}(1,2),(a_j^{(l)}+A_j^{(l)},A_j^{(l)})_{j=1:p_l}\\(b_j^{(l)}+B_j^{(l)},B_j^{(l)})_{j=1:q_l}\end{matrix}\right]_{l=1:L}\right)$
SC	$\mathcal{I}_{c0}(\mathrm{b})=\frac{K}{\Lambda}H^{0,1:[m_l,n_l+1]_{l=1:L}}_{1,0:[p_l+1,q_l+1]_{l=1:L}}\left(\begin{matrix}\lambda_1/\mathrm{b}\\\vdots\\\lambda_L/\mathrm{b}\end{matrix}\middle\vert\begin{matrix}(0:\{1\}_{l=1:L})\\-\end{matrix}\quad\left[\begin{matrix}(1,1),(a_j^{(l)}+A_j^{(l)},A_j^{(l)})_{j=1:p_l}\\(b_j^{(l)}+B_j^{(l)},B_j^{(l)})_{j=1:q_l},(0,1)\end{matrix}\right]_{l=1:L}\right)$
	$\mathcal{I}_{c1}(\mathrm{b})=\frac{K/\Lambda}{\sqrt{\mathrm{b}}}H^{0,1:[m_l,n_l+1]_{l=1:L}}_{1,0:[p_l+1,q_l+1]_{l=1:L}}\left(\begin{matrix}\lambda_1/\mathrm{b}\\\vdots\\\lambda_L/\mathrm{b}\end{matrix}\middle\vert\begin{matrix}(\frac{1}{2}:\{1\}_{l=1:L})\\-\end{matrix}\quad\left[\begin{matrix}(1,1),(a_j^{(l)}+A_j^{(l)},A_j^{(l)})_{j=1:p_l}\\(b_j^{(l)}+B_j^{(l)},B_j^{(l)})_{j=1:q_l},(0,1)\end{matrix}\right]_{l=1:L}\right)$
	$\mathcal{I}_{c2}(\mathrm{a},\mathrm{b})=\frac{K/\Lambda}{2\sqrt{\pi\mathrm{b}}}H^{0,1:(1,1),[m_l,n_l+1]_{l=1:L}}_{1,0:(1,2),[p_l+1,q_l+1]_{l=1:L}}\left(\begin{matrix}\mathrm{a}/2\mathrm{b}\\\lambda_1/\mathrm{b}\\\vdots\\\lambda_L/\mathrm{b}\end{matrix}\middle\vert\begin{matrix}(\frac{1}{2}:1,\{1\}_{l=1:L})\\-\end{matrix}\quad\begin{matrix}(1,1)\\(\frac{1}{2},1),(0,1)\end{matrix}\quad\left[\begin{matrix}(1,1),(a_j^{(l)}+A_j^{(l)},A_j^{(l)})_{j=1:p_l}\\(b_j^{(l)}+B_j^{(l)},B_j^{(l)})_{j=1:q_l},(0,1)\end{matrix}\right]_{l=1:L}\right)$

again into [15, Tab. III] yields the asymptotic expressions for the SER.

$$\mathcal{I}_{c0}(\mathrm{b})\sim\frac{\frac{K}{\Lambda}}{\eta_1^{L-1}}\frac{\Gamma\left(L-\sum_{l=1}^{L}s_l^*\right)}{\Gamma\left(\frac{L}{\eta_1}-\frac{1}{\eta_1}\sum_{l=1}^{L}s_l^*\right)}\prod_{l=1}^{L}E_{j_l}^{(l)}\Gamma\left(\frac{1-s_l^*}{\eta_1}\right)\times\left[\ln\left(\frac{\mathrm{b}}{\lambda_l}\right)\right]^{N_{j_l}^{(l)}-1}\left(\frac{\lambda_l}{\eta_0\mathrm{b}}\right)^{1-s_l^*} \tag{41a}$$

$$\mathcal{I}_{c1}(\mathrm{b})\sim\frac{\frac{K}{\Lambda}}{\eta_1^{L}\sqrt{\mathrm{b}}}\frac{\Gamma\left(L+\frac{1}{2}-\sum_{l=1}^{L}s_l^*\right)}{\Gamma\left(1+\frac{L}{\eta_1}-\frac{1}{\eta_1}\sum_{l=1}^{L}s_l^*\right)}\prod_{l=1}^{L}E_{j_l}^{(l)}\Gamma\left(\frac{1-s_l^*}{\eta_1}\right)\times\left[\ln\left(\frac{\mathrm{b}}{\lambda_l}\right)\right]^{N_{j_l}^{(l)}-1}\left(\frac{\lambda_l}{\eta_0\mathrm{b}}\right)^{1-s_l^*} \tag{41b}$$

$$\mathcal{I}_{c2}(\mathrm{a},\mathrm{b})\sim\frac{\frac{\sqrt{\mathrm{a}}K}{\Lambda}}{\eta_1^{L}\mathrm{b}\sqrt{2\pi}}\frac{\Gamma\left(L+1-\sum_{l=1}^{L}s_l^*\right)}{\Gamma\left(1+\frac{L}{\eta_1}-\frac{1}{\eta_1}\sum_{l=1}^{L}s_l^*\right)}{}_2F_1\left(\frac{1}{2},L+1-\sum_{l=1}^{L}s_l^*;\frac{3}{2};-\frac{\mathrm{a}}{2\mathrm{b}}\right)\prod_{l=1}^{L}E_{j_l}^{(l)}\Gamma\times\left(\frac{1-s_l^*}{\eta_1}\right)\left[\ln\left(\frac{\mathrm{b}}{\lambda_l}\right)\right]_{j_l}^{N^{(l)}-1}\left(\frac{\lambda_l}{\eta_0\mathrm{b}}\right)^{1-s_l^*} \tag{41c}$$

C. Demonstrative Examples

It is of interest to demonstrate how the proposed framework will allow us to derive exact expressions and asymptotic expansions for the SER for the different fading channels and the aforementioned diversity receivers. Due to space limitations, we find it difficult to list all the possible combinations for all cases. Moreover, we see it is more constructive to demonstrate how the proposed framework can be used to derive results of interest for nontrivial cases, which have not been treated before in the literature. In the following examples, we assume all the fading branches to be statistically independent.

1) Example 1—$\alpha-\mu$ Fading With SC Diversity and M-ary PSK Modulation: According to [15, Tab. III], the SER for PSK modulation is given by

$$P_e=\frac{\sin\frac{\pi}{M}}{\sqrt{\pi}}\left[\frac{1}{2}\mathcal{I}_{c1}\left(\sin^2\left(\frac{\pi}{M}\right)\right)+\mathcal{I}_{c2}\left(2\cos^2\left(\frac{\pi}{M}\right),\sin^2\left(\frac{\pi}{M}\right)\right)\right]. \tag{42}$$

The expressions for $\mathcal{I}_{c1}(\cdot)$ and $\mathcal{I}_{c2}(\cdot)$ are obtained by substituting the $\alpha-\mu$ parameters into the eighth and ninth rows of Table VII, respectively. Substituting the result into (42) while setting $\mathrm{a}=2\cos^2(\pi/M)$ and $\mathrm{b}=\sin^2(\pi/M)$ yields the exact expression for the SER shown in (43), shown at the bottom of the next page. In this expression, $\beta_l=(\Gamma(\mu+1/\alpha_l)/\Gamma(\mu_l))$,

TABLE VIII
ASYMPTOTIC EXPANSIONS FOR $\mathcal{I}_{c0}(\mathrm{b})$, $\mathcal{I}_{c1}(\mathrm{b})$, AND $\mathcal{I}_{c2}(\mathrm{a},\mathrm{b})$ FOR DIFFERENT DIVERSITY COMBINING RECEIVERS SUBJECT TO FOX'S H-FUNCTION CHANNEL FADING. SIMPLE POLES OF $f^*(\mathrm{s})$ ARE ASSUMED. $K=\prod_{l=1}^{L}\kappa_l$ AND $\Lambda=\prod_{l=1}^{L}\lambda_l$

Diversity	Expressions for $\mathcal{I}_{c0}(\mathrm{b})$, $\mathcal{I}_{c1}(\mathrm{b})$, and $\mathcal{I}_{c2}(\mathrm{a},\mathrm{b})$
MRC	$\mathcal{I}_{c0}(\mathrm{b}) \sim \frac{K}{\Lambda}\prod_{l=1}^{L} E_{j_l}^{(l)}\Gamma\left(1-s_l^*\right)\left[\ln\left(\frac{\mathrm{b}}{\lambda_l}\right)\right]^{N_{j_l}^{(l)}-1}\left(\frac{\lambda_l}{\mathrm{b}}\right)^{1-s_l^*}$ $\mathcal{I}_{c1}(\mathrm{b}) \sim \frac{K/\Lambda}{\sqrt{\mathrm{b}}}\left[\frac{\Gamma\left(L+\frac{1}{2}-\sum_{l=1}^{L}s_l^*\right)}{\Gamma\left(1+L-\sum_{l=1}^{L}s_l^*\right)}\prod_{l=1}^{L} E_{j_l}^{(l)}\Gamma\left(1-s_l^*\right)\left[\ln\left(\frac{\mathrm{b}}{\lambda_l}\right)\right]^{N_{j_l}^{(l)}-1}\left(\frac{\lambda_l}{\mathrm{b}}\right)^{1-s_l^*}\right]$ $\mathcal{I}_{c2}(\mathrm{a},\mathrm{b}) \sim \frac{\sqrt{\mathrm{a}}K/\Lambda}{\mathrm{b}\sqrt{2\pi}}\left[{}_2F_1\left(\frac{1}{2},L+1-\sum_{l=1}^{L}s_l^*;\frac{3}{2};-\frac{\mathrm{a}}{2\mathrm{b}}\right)\prod_{l=1}^{L} E_{j_l}^{(l)}\Gamma\left(1-s_l^*\right)\left[\ln\left(\frac{\mathrm{b}}{\lambda_l}\right)\right]^{N_{j_l}^{(l)}-1}\left(\frac{\lambda_l}{\mathrm{b}}\right)^{1-s_l^*}\right]$
EGC	$\mathcal{I}_{c0}(\mathrm{b}) \sim \sqrt{\pi}\frac{K}{\Lambda}\frac{1}{\Gamma\left(L+\frac{1}{2}-\sum_{l=1}^{L}s_l^*\right)}\prod_{l=1}^{L} 2E_{j_l}^{(l)}\Gamma\left(2-2s_l^*\right)\left[\ln\left(\frac{\mathrm{b}}{\lambda_l}\right)\right]^{N_{j_l}^{(l)}-1}\left(\frac{L\lambda_l}{4\mathrm{b}}\right)^{1-s_l^*}$ $\mathcal{I}_{c1}(\mathrm{b}) \sim \sqrt{\frac{\pi}{\mathrm{b}}}\frac{K}{\Lambda}\left[\frac{1}{\Gamma\left(L+1-\sum_{l=1}^{L}s_l^*\right)}\prod_{l=1}^{L} 2E_{j_l}^{(l)}\Gamma\left(2-2s_l^*\right)\left[\ln\left(\frac{\mathrm{b}}{\lambda_l}\right)\right]^{N_{j_l}^{(l)}-1}\left(\frac{L\lambda_l}{4\mathrm{b}}\right)^{1-s_l^*}\right]$ $\mathcal{I}_{c2}(\mathrm{a},\mathrm{b}) \sim \frac{\sqrt{\mathrm{a}}}{\mathrm{b}\sqrt{2}}\frac{K}{\Lambda}\left[\frac{{}_2F_1\left(\frac{1}{2},L+1-\sum_{l=1}^{L}s_l^*;\frac{3}{2};-\frac{\mathrm{a}}{2\mathrm{b}}\right)}{\Gamma\left(L+\frac{1}{2}-\sum_{l=1}^{L}s_l^*\right)}\prod_{l=1}^{L} 2E_{j_l}^{(l)}\Gamma\left(2-2s_l^*\right)\left[\ln\left(\frac{\mathrm{b}}{\lambda_l}\right)\right]^{N_{j_l}^{(l)}-1}\left(\frac{L\lambda_l}{4\mathrm{b}}\right)^{1-s_l^*}\right]$
SC	$\mathcal{I}_{c0}(\mathrm{b}) \sim \frac{K}{\Lambda}\left[\Gamma\left(L+1-\sum_{l=1}^{L}s_l^*\right)\prod_{l=1}^{L}\frac{E_{j_l}^{(l)}}{1-s_l^*}\left[\ln\left(\frac{\mathrm{b}}{\lambda_l}\right)\right]^{N_{j_l}^{(l)}-1}\left(\frac{\lambda_l}{\mathrm{b}}\right)^{1-s_l^*}\right]$ $\mathcal{I}_{c1}(\mathrm{b}) \sim \frac{1}{\sqrt{\mathrm{b}}}\frac{K}{\Lambda}\left[\Gamma\left(L+\frac{1}{2}-\sum_{l=1}^{L}s_l^*\right)\prod_{l=1}^{L}\frac{E_{j_l}^{(l)}}{1-s_l^*}\left[\ln\left(\frac{\mathrm{b}}{\lambda_l}\right)\right]^{N_{j_l}^{(l)}-1}\left(\frac{\lambda_l}{\mathrm{b}}\right)^{1-s_l^*}\right]$ $\mathcal{I}_{c2}(\mathrm{a},\mathrm{b}) \sim \frac{\sqrt{\mathrm{a}}}{\mathrm{b}\sqrt{2\pi}}\frac{K}{\Lambda}\left[\Gamma\left(L+1-\sum_{l=1}^{L}s_l^*\right){}_2F_1\left(\frac{1}{2},L+1-\sum_{l=1}^{L}s_l^*;\frac{3}{2};-\frac{\mathrm{a}}{2\mathrm{b}}\right)\prod_{l=1}^{L}\frac{E_{j_l}^{(l)}}{1-s_l^*}\left[\ln\left(\frac{\mathrm{b}}{\lambda_l}\right)\right]^{N_{j_l}^{(l)}-1}\left(\frac{\lambda_l}{\mathrm{b}}\right)^{1-s_l^*}\right]$

$l=1,\ldots,L$. For the asymptotic expansions, the basic functions $\mathcal{I}_{c1}(\cdot)$ and $\mathcal{I}_{c2}(\cdot)$ are obtained using the eighth and ninth rows of Table VIII, respectively. Since $m_l=1$, $l=1,\ldots,L$, we have $N_{j_l}^{(l)}=1$ and $E_{j_l}^{(l)}=\alpha_l$ for all l and j_l. The final asymptotic expression for the SER will be as given in (44), shown at the bottom of the page.

2) Example 2—EGK Fading With EGC Diversity and M-QAM Modulation: According to [15, Tab. III], the exact SER for M-QAM modulation is given by

$$P_e=\frac{\sqrt{M}-1}{\sqrt{M}}\sqrt{\frac{6}{\pi(M-1)}}\times\left[\frac{1}{\sqrt{M}}\mathcal{I}_{c1}\left(\frac{3}{2(M-1)}\right)+2\frac{\sqrt{M}-1}{\sqrt{M}}\mathcal{I}_{c2}\left(\frac{3}{M-1},\frac{3}{2(M-1)}\right)\right] \tag{45}$$

$$P_e=\frac{1}{2\sqrt{\pi}\prod_{l=1}^{L}\Gamma(\mu_l)}\left[H_{1,0:[1,2]_{l=1:L}}^{0,1:[1,1]_{l=1:L}}\left(\begin{array}{c}\frac{\beta_1}{\sin^2\left(\frac{\pi}{M}\right)\bar{\gamma}_1}\\ \vdots\\ \frac{\beta_L}{\sin^2\left(\frac{\pi}{M}\right)\bar{\gamma}_L}\end{array}\middle|\begin{array}{c}\left(\frac{1}{2}:\{1\}_{l=1:L}\right)\\ -\end{array}\quad\left[\begin{array}{c}(1,1)\\ \left(\mu_l,\frac{1}{\alpha_l}\right),(0,1)\end{array}\right]_{l=1:L}\right)\right.$$
$$\left.+\frac{1}{\sqrt{\pi}}H_{1,0:(1,2),[1,2]_{l=1:L}}^{0,1:(1,1),[1,1]_{l=1:L}}\left(\begin{array}{c}\cot^2\left(\frac{\pi}{M}\right)\\ \frac{\beta_1}{\sin x^2\left(\frac{\pi}{M}\right)\bar{\gamma}_1}\\ \vdots\\ \frac{\beta_L}{\sin^2\left(\frac{\pi}{M}\right)\bar{\gamma}_L}\end{array}\middle|\begin{array}{c}\left(\frac{1}{2}:1,\{1\}_{l=1:L}\right)\\ -\end{array}\quad\begin{array}{c}(1,1)\\ \left(\frac{1}{2},1\right),(0,1)\end{array}\left[\begin{array}{c}(1,1)\\ \left(\mu_l,\frac{1}{\alpha_l}\right),(0,1)\end{array}\right]_{l=1:L}\right)\right] \tag{43}$$

$$P_e\sim\frac{1}{\sqrt{\pi}}\prod_{l=1}^{L}\frac{1}{\Gamma(1+\mu_l)}\left(\frac{\beta_l}{\sin^2\left(\frac{\pi}{M}\right)\bar{\gamma}_l}\right)^{\alpha_l\mu_l}\times\left[\frac{1}{2}\Gamma\left(\frac{1}{2}+\sum_{l=1}^{L}\alpha_l\mu_l\right)+\frac{\cot\left(\frac{\pi}{M}\right)}{\sqrt{\pi}}\Gamma\left(1+\sum_{l=1}^{L}\alpha_l\mu_l\right){}_2F_1\left(\frac{1}{2},1+\sum_{l=1}^{L}\alpha_l\mu_l;\frac{3}{2};-\cot^2\left(\frac{\pi}{M}\right)\right)\right]. \tag{44}$$

where, in this case, the basic functions $\mathcal{I}_{c1}(\cdot)$ and $\mathcal{I}_{c2}(\cdot)$ are given by the fifth and sixth rows of Table VII. Hence, the final expression for the SER is given by setting $\mathrm{a} = 3/(M-1)$ and $\mathrm{b} = 3/2(M-1)$ in $\mathcal{I}_{c1}(\cdot)$ and $\mathcal{I}_{c2}(\cdot)$ then substituting into (45), yielding the result in (46), shown at the bottom of the page. Finally, the asymptotic expansion of the SER can be easily obtained using Theorem 2 with m'_l, $E^{(l)}_{j_l}$, and $N^{(l)}_{j_l}$ being as defined in Section II-D2. Defining $\mu_{1,l} = \mu_l$, $\mu_{2,l} = \mu_{sl}$, $\xi_{1,l} = \xi_l$, $\xi_{2,l} = \xi_{sl}$, $l = 1, \ldots, L$, and $j_l = \arg\max_{j=1,2} \mu_{j,1}\xi_{j,l}$, the asymptotic expansion of the SER is given by (47), shown at the bottom of the page.

IV. Numerical and Simulation Results

Here, we compare the values of the SER obtained via Monte Carlo simulations with our derived exact and asymptotic expressions for single-branch communications as well as MRC, EGC, and SC diversity receivers to illustrate the accuracy of the presented mathematical formulation. Furthermore, we compare the exact and the asymptotic results for the capacity expressions for single-branch communications. In most of the results, we consider the EGK fading distribution and special cases of it as representative examples. The solid lines in all figures denote the exact results, whereas the dashed ones represent the asymptotic results. The markers denote the simulation results, which are obtained using MATLAB.

We first start with the SER for single-branch receivers. In Fig. 2, we consider communications using QPSK, CBFSK, and DBPSK over Weibull and Nakagami-m fading channels while 8-PSK, 8-QAM, and 8-NCFSK modulation schemes operating over the generalized-K and the Weibull–Gamma composite fading channels are considered in Fig. 3. Furthermore, the SER for the single-branch case is shown in Fig. 4 for 16-symbol systems considering different combinations of the EGK channel parameters. In all the figures, we notice a strong match between the exact and simulation results of the SER for all the SNR ranges. Moreover, we notice that the exact and asymptotic expansions agree very well at high SNRs. This

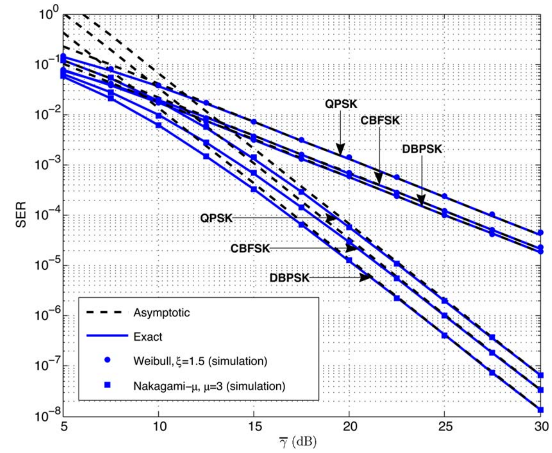

Fig. 2. Exact, asymptotic, and simulated SER results of QPSK, CBFSK, and DBPSK modulation schemes over some limiting cases of the EGK fading model.

$$P_e = \frac{2^{L+1}(\sqrt{M}-1)}{M\pi \prod_{l=1}^{L}\Gamma(\mu_l)\Gamma(\mu_{sl})} \times \left[H^{0,0:[2,1]_{l=1:L}}_{0,1:[1,2]_{l=1:L}} \left(\begin{matrix} \frac{L(M-1)\beta_{s1}\beta_1}{6\bar{\gamma}_1} \\ \vdots \\ \frac{L(M-1)\beta_{sL}\beta_L}{6\bar{\gamma}_L} \end{matrix} \,\middle|\, \begin{matrix} - \\ (0:\{1\}_{l=1:L}) \end{matrix} \quad \left[\begin{matrix} (1,2) \\ \left(\mu_l - \frac{1}{\xi_l}, \frac{1}{\xi_l}\right), \left(\mu_{sl} - \frac{1}{\xi_{sl}}, \frac{1}{\xi_{sl}}\right) \end{matrix}\right]_{l=1:L} \right) \right.$$
$$\left. + \frac{\sqrt{M}-1}{\pi} H^{0,1:(1,1),[2,1]_{l=1:L}}_{1,1:(1,2),[1,2]_{l=1:L}} \times \left(\begin{matrix} \frac{1}{\frac{2(M-1)\beta_1\beta_{s1}L}{3\bar{\gamma}_1}} \\ \vdots \\ \frac{2(M-1)\beta_L\beta_{sL}L}{3\bar{\gamma}_L} \end{matrix} \,\middle|\, \begin{matrix} \left(\frac{1}{2}:1,\{1\}_{l=1:L}\right) \\ \left(0:0,\{2\}_{l=1:L}\right) \end{matrix} \quad \begin{matrix} (1,1) \\ \left(\frac{1}{2},1\right),(0,1) \end{matrix} \quad \left[\begin{matrix} (1,2) \\ \left(\mu_l - \frac{1}{\xi_l}, \frac{1}{\xi_l}\right), \left(\mu_{sl} - \frac{1}{\xi_{sl}}, \frac{1}{\xi_{sl}}\right) \end{matrix}\right]_{l=1:L} \right) \right] \tag{46}$$

$$P_e \sim \frac{2(\sqrt{M}-1)}{\sqrt{M}} \left(\prod_{l=1}^{L} \frac{E^{(l)}_j \Gamma\left(1 + 2\mu_{j_l,l}\xi_{j_l,l}\right)}{\xi_{j_l,l}\Gamma\left(\mu_{3-j_l,l}\right)\Gamma\left(1+\mu_{j_l,l}\right)} \left[\ln\left(\frac{3\bar{\gamma}_l}{2(M-1)\beta_l\beta_{sl}}\right)\right]^{N^{(l)}_j - 1} \left(\frac{L(M-1)\beta_l\beta_{sl}}{6\bar{\gamma}_l}\right)^{\mu_{j_l,l}\xi_{j_l,l}} \right)$$
$$\times \left[\frac{1}{\sqrt{M}\Gamma\left(1 + \sum_{l=1}^{L}\mu_{j_l,l}\xi_{j_l,l}\right)} + 2\frac{\sqrt{M}-1}{\sqrt{M\pi}} \frac{{}_2F_1\left(\frac{1}{2}, 1 + \sum_{l=1}^{L}\mu_{j_l,l}\xi_{j_l,l}; \frac{3}{2}; -1\right)}{\Gamma\left(\frac{1}{2} + \sum_{l=1}^{L}\mu_{j_l,l}\xi_{j_l,l}\right)} \right] \tag{47}$$

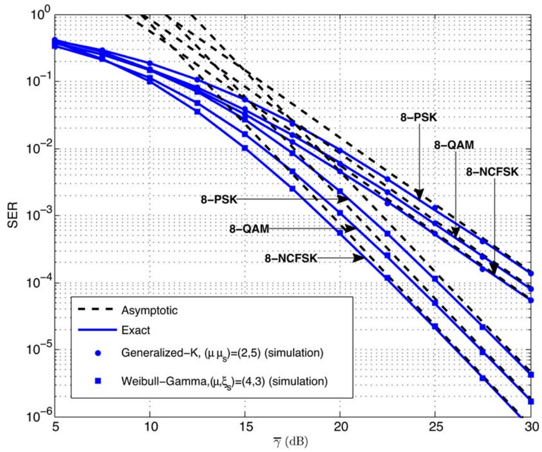

Fig. 3. Exact, asymptotic, and simulated SER results of 8-PSK, 8-QAM, and 8-NCFSK over some special cases of the EGK fading model.

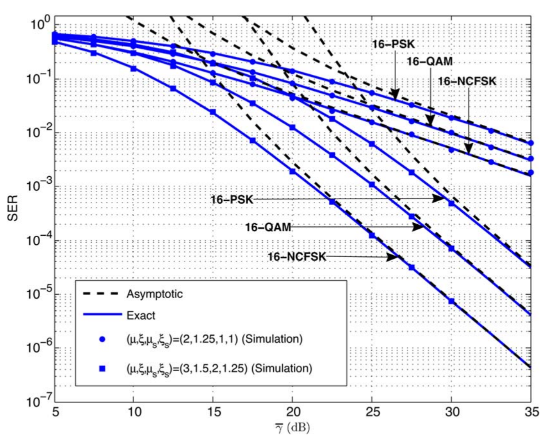

Fig. 4. Exact, asymptotic, and simulated SER performance considering 16-PSK, 16-QAM, and 16-NCFSK over EGK fading with different parameters.

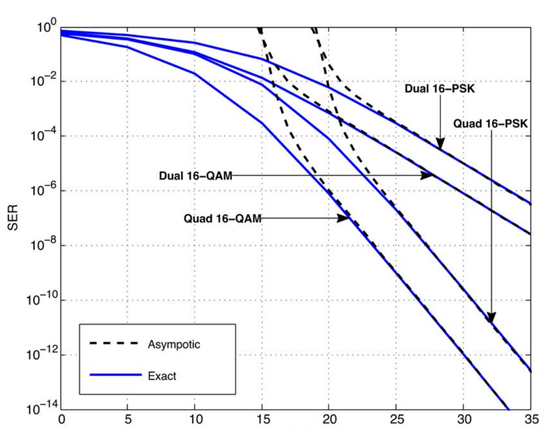

Fig. 5. SER for dual- and quad-branch MRC receivers employing 16-PSK and 16-QAM with $\mu_l = 1$, $\xi_l = 1.5$, $\mu_{sl} = 3.5$, and $\xi_{sl} = 2$.

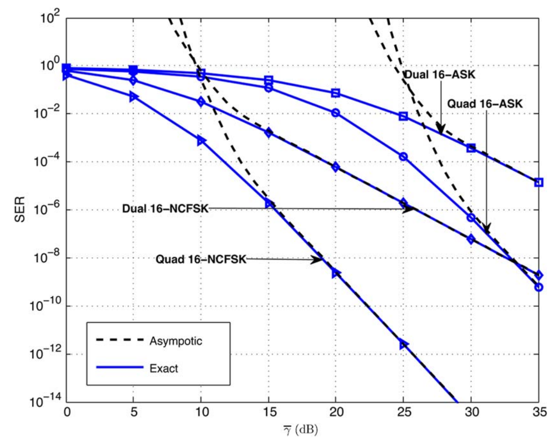

Fig. 6. SER for dual- and quad-branch EGC receivers employing 16-ASK and 16-NCFSK with $\mu_l = 1$, $\xi_l = 1.5$, $\mu_{sl} = 3.5$, and $\xi_{sl} = 2$.

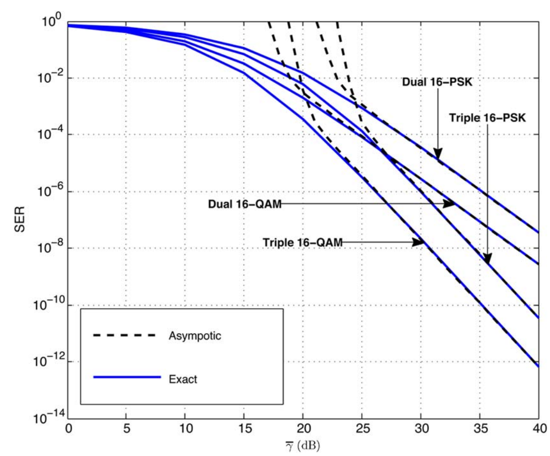

Fig. 7. SER for dual- and triple-branch SC receivers employing 16-PSK and 16-QAM with $\mu_l = 1$, $\xi_l = 1.5$, $\mu_{sl} = 3.5$, and $\xi_{sl} = 2$.

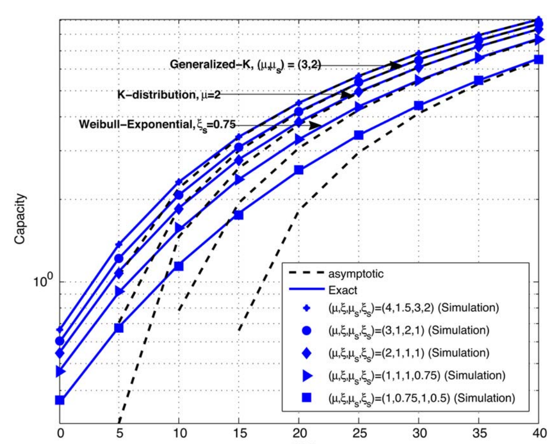

Fig. 8. Exact, asymptotic, and simulated capacity over EGK composite fading assuming different distribution parameters.

confirms the validity of our mathematical analysis for different communication scenarios and parameter settings. It is important to note that the asymptotic expansions are much easier and faster to calculate than the exact SER values and are not prone to underflow usually encountered in numerical integration when very small values SER are calculated. This is the reason behind the strength of using the asymptotic expansions for quickly comparing different communication scenarios.

The applicability of our proposed framework for computing the SER of MRC, EGC, and SC diversity receivers is next

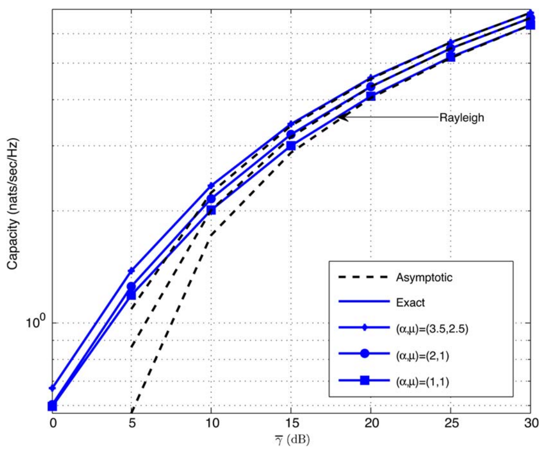

Fig. 9. Exact, asymptotic, and simulated capacity over $\alpha-\mu$ fading assuming different distribution parameters.

demonstrated in Figs. 5–7, respectively. In these figures, all branches are assumed to be statistically independent and are subject to identical EGK fading distribution with the following channel parameters: $\mu_l = 1$, $\xi_l = 1.5$, $\mu_{sl} = 3.5$, and $\xi_{sl} = 2$. In Figs. 5 and 6, we consider dual- and quad-branch diversity receivers, respectively, whereas in Fig. 7, dual- and triple-branch receivers are considered. Different modulation schemes are also considered. As shown in these three figures, the asymptotic results match the exact results well at high average SNR. Furthermore, as expected, the average SER decreases significantly with the increase in the number of diversity branches.

We next demonstrate the capacity of special cases of the H-function distribution. In Figs. 8 and 9, the capacity of the EGK and $\alpha-\mu$ fading channels, respectively, is depicted. As before, a strong match between the exact and asymptotic values of the capacity for SNR values roughly above 25 dB can be noticed in both figures. Moreover, the match increases for less severely faded channels in which the values of α or ξ are relatively smaller than μ. We also notice that, in all cases, the value of the asymptotic capacity is always less than its corresponding exact one. Hence, we may argue that the obtained asymptotic expression may serve as a *tight* lower bound for the true capacity.

V. Conclusion

In this paper, we have evaluated the performance of single- and multiple-branch diversity receivers when operating over Fox's H-function fading channel as a unified fading model that subsumes many fading models of practical interest. For single-branch communications, we have derived exact expressions and asymptotic expansions for the SER and the channel capacity, whereas for multiple-branch communications, only exact SER analysis was addressed. Our mathematical analysis was validated by various computer simulations considering a variety of special fading distributions, modulation schemes, and diversity receivers. In all experiments, a perfect match between the exact expressions and their corresponding asymptotic expansions has been clearly observed.

Appendix A
Python Implementation of the Multivariate H-Function

```python
from __future__ import division
import numpy as np
import scipy.special as special
import itertools
def detBoundaries(params, tol):
   '''Determine rectangular boundaries of
       integration region of Fox-H function.'''
   boundary_range = np.arange(0, 50, 0.05)
   dims = len(params[0])
   boundaries = np.zeros(dims)
   for dim_l in range(dims):
      points = np.zeros((boundary_range.shape[0],
          dims))
      points[:, dim_l] = boundary_range
      abs_integrand = np.abs(compMultiFoxHIntegrand
                        (points, params))
      index = np.max(np.nonzero(abs_integrand>
          tol*abs_integrand[0]))
      boundaries[dim_l] = boundary_range[index]
   return boundaries
def compMultiFoxHIntegrand(y, params):
   ''' Compute complex integrand of Fox-H function
       at points given by rows of matrix y.'''
   z, mn, pq, c, d, a, b = params
   m, n = zip(*mn)
   p, q = zip(*pq)
   npoints, dims = y.shape
   s = 1j*y
   lower = np.zeros(dims)
   upper = np.zeros(dims)
   for dim_l in range(dims):
      if b[dim_l]:
         bj, Bj = zip(*b[dim_l])
         bj = np.array(bj[:m[dim_l+1]])
         Bj = np.array(Bj[:m[dim_l+1]])
         lower[dim_l] = -np.min(bj/Bj)
      else:
         lower[dim_l] = -100
      if a[dim_l]:
         aj, Aj = zip(*a[dim_l])
         aj = np.array(aj[:n[dim_l+1]])
         Aj = np.array(Aj[:n[dim_l+1]])
         upper[dim_l] = np.min((1-aj)/Aj)
      else:
         upper[dim_l] = 0
   mindist = np.linalg.norm(upper-lower)
   sigs = 0.5*(upper+lower)
   for j in range(n[0]):
      num = 1 - c[j][0] - np.sum(c[j][1:] * lower)
      cnorm = np.linalg.norm(c[j][1:])
      newdist = np.abs(num) / cnorm
      if newdist < mindist:
         mindist = newdist
         sigs = lower +
             0.5*num*np.array(c[j][1:])/(cnorm*cnorm)
   s += sigs
   s1 = np.c_[np.ones((npoints, 1)), s]
   prod_gam_num = prod_gam_denom = 1+0j
   for j in range(n[0]):
      prod_gam_num *= special.gamma(1-np.dot(s1,
          c[j]))
   for j in range(q[0]):
      prod_gam_denom *= special.gamma(1-np.dot(s1,
          d[j]))
   for j in range(n[0], p[0]):
      prod_gam_denom *=
          special.gamma(np.dot(s1,c[j]))
   for dim_l in range(dims):
      for j in range(n[dim_l+1]):
         prod_gam_num *= special.gamma(1 -
             a[dim_l][j][0] - a[dim_l][j][1]*s[:,
             dim_l])
      for j in range(m[dim_l+1]):
         prod_gam_num *=
             special.gamma(b[dim_l][j][0] +
             b[dim_l][j][1]*s[:, dim_l])
      for j in range(n[dim_l+1], p[dim_l+1]):
         prod_gam_denom *=
             special.gamma(a[dim_l][j][0] +
             a[dim_l][j][1]*s[:, dim_l])
      for j in range(m[dim_l+1], q[dim_l+1]):
         prod_gam_denom *= special.gamma(1 -
             b[dim_l][j][0] - b[dim_l][j][1]*s[:,
             dim_l])
   zs = np.power(z, -s)
   result =
       (prod_gam_num/prod_gam_denom)*np.prod(zs,
       axis=1)/(2*np.pi)**dims
   return result
def compMultiFoxH(params, nsubdivisions,
    boundaryTol=0.0001):
   '''Estimate multivariate integral using
       rectangular quadrature.
   Inputs: 'params': list containing z, mn, pq, c,
       d, a, b. 'nsubdivisions': the number of
       divisions taken along each dimension.
       'boundaryTol': tolerance used for
       determining the boundaries. Output:
       'result': the estimated value of the Fox H
       function...'''
   boundaries = detBoundaries(params, boundaryTol)
   dim = boundaries.shape[0]
   signs = list(itertools.product([1,-1],
       repeat=dim))
   code = list(itertools.product(range
             (int(nsubdivisions/2)), repeat=dim))
   quad = 0
   res = np.zeros((0))
   for sign in signs:
      points = np.array(sign)*(np.array(code)+0.5)
             *boundaries*2/nsubdivisions
      res = np.r_[res,np.real(compMultiFoxHIntegrand
                (points, params))]
      quad += np.sum(compMultiFoxHIntegrand(points,
          params))
   volume = np.prod(2*boundaries/nsubdivisions)
   result = quad*volume
   return result
```

$$f_\gamma(\gamma) = \begin{cases} A^{(G)} \sum_{k=1}^{\infty} a_k^{(G)} \gamma^{\frac{(\alpha+k)}{2}} K_{\alpha-k}\left(2\sqrt{\frac{\alpha\gamma}{I}}\right), & \text{if } \beta \text{ is non-integer} \\ A \sum_{k=1}^{\beta} a_k \gamma^{\frac{(\alpha+k)}{2}} K_{\alpha-k}\left(2\sqrt{\frac{\alpha\beta\gamma}{I\beta+\Omega'}}\right), & \text{if } \beta \text{ is an integer} \end{cases} \tag{50}$$

$$f_\gamma(\gamma) = \begin{cases} \frac{1}{2} A^{(G)} \sum_{k=1}^{\infty} a_k^{(G)} H_{0,2}^{2,0}\left(\frac{\alpha}{I}\gamma \,\middle|\, \begin{matrix} - \\ \left(\frac{\nu+\alpha+k}{2}, 1\right), \left(\frac{-\nu+\alpha+k}{2}, 1\right) \end{matrix}\right) & \text{if } \beta \text{ is non-integer} \\ \frac{1}{2} A \sum_{k=1}^{\beta} a_k H_{0,2}^{2,0}\left(\frac{\alpha\beta}{I\beta+\Omega'}\gamma \,\middle|\, \begin{matrix} - \\ \left(\frac{\nu+\alpha+k}{2}, 1\right), \left(\frac{-\nu+\alpha+k}{2}, 1\right) \end{matrix}\right) & \text{if } \beta \text{ is an integer.} \end{cases} \tag{51}$$

APPENDIX B
GAMMA–GAMMA AND THE MÁLAGA DISTRIBUTIONS AS SPECIAL CASES OF THE FOX'S H-FUNCTION FADING MODEL

The gamma–gamma and the Málaga distributions have been presented in the literature to describe the fading phenomenon over FSO channels. Let us start with the gamma–gamma distribution. According to [6], the pdf of the instantaneous SNR is given by [6, Eq. (3)]

$$f_\gamma(\gamma) = \frac{\xi^2}{r\gamma\Gamma(\alpha)\Gamma(\beta)} G_{1,3}^{3,0}\left(\alpha\beta\left(\frac{\gamma}{\mu_{RD}}\right)^{\frac{1}{r}} \,\middle|\, \begin{matrix} \xi^2+1 \\ \xi^2, \alpha, \beta \end{matrix}\right) \tag{48}$$

where $\alpha, \beta, \xi, r, \mu_{RD}$ are some properly defined parameters related to the FSO link. Since the Meijer-G function is a special case of the Fox-H function [21, Eq. (1.112)] and using the relations in [21, Eqs. (1.59) and (1.60)], the instantaneous SNR pdf can be written as

$$f_\gamma(\gamma) = \frac{\xi^2}{\Gamma(\alpha)\Gamma(\beta)} \times H_{1,3}^{3,0}\left(\frac{(\alpha\beta)^r}{\mu_{RD}}\gamma \,\middle|\, \begin{matrix} \left(\xi^2+1-r, r\right) \\ \left(\xi^2-r, r\right), (\alpha-r, r), (\beta-r, r) \end{matrix}\right) \tag{49}$$

which is indeed a special case of the model considered in this paper. Note that the ROC of the Mellin transform is $\Re\{s\} > 1 - \min(\alpha, \beta, \xi^2)/r$, which is guaranteed to include the point $s = 1$ as long as α, β, r are positive. Moreover, the expressions for the SER and capacity can be obtained by setting $\kappa = (\xi^2/\Gamma(\alpha)\Gamma(\beta))$, $\lambda = ((\alpha\beta)^r/\mu_{RD})$, $m = q = 3$, $n = 0$, $p = 1$, $a_1 = \xi^2 + 1 - r$, $b_1 = \xi^2 - r$, $b_2 = \alpha - r$, $b_3 = \beta - r$, and $A_1 = B_1 = B_2 = B_3 = r$.

Regarding the Málaga distribution, according to [7], the SNR pdf is given by (50), shown at the top of the page, where α, β, I, Ω' are the distribution parameters; A, $A^{(G)}$, a_k, and $a_k^{(G)}$ are some dependent constants; and $K_\nu(\cdot)$ is the modified Bessel function of the second kind. The modified Bessel function can be expressed in terms of the Meijer's G-function as in [24, Eq. (9.34.3)], which can readily be written in terms of the H-function using [21, Eq. (1.112)]. Thus, the pdf can be represented as the sum of the Fox-H functions given in (51), shown at the top of the page. Thus, if β is not integer, the SER and the ergodic capacity should be an infinite series in which the kth term corresponds to $\kappa = (1/2)A^{(G)}a_k^{(G)}$, $\lambda = \alpha/I$, $m = q = 2$, $n = p = 0$, $b_1 = (\nu + \alpha + k)/2$, $b_2 = (-\nu + \alpha + k)/2$, and $B_1 = B_2 = 1$. If β is an integer, the SER and the ergodic capacity should be a finite series of $\beta + 1$ terms in which the kth term corresponds to $\kappa = (1/2)Aa_k$, $\lambda = \alpha\beta/(I\beta + \Omega')$, $m = q = 2$, $n = p = 0$, $b_1 = (\nu + \alpha + k)/2$, $b_2 = (-\nu + \alpha + k)/2$, and $B_1 = B_2 = 1$.

REFERENCES

[1] M. K. Simon and M.-S. Alouini, *Digital Communication Over Fading Channels*. Hoboken, NJ, USA: Wiley, 2005.
[2] M. D. Yacoub, "The $\alpha - \mu$ distribution: A physical fading model for the Stacy distribution," *IEEE Trans. Veh. Technol.*, vol. 56, no. 11, pp. 27–34, Jan. 2007.
[3] A. Abdi and M. Kaveh, "K distribution: An appropriate substitute for Rayleigh-lognormal distribution in fading-shadowing wireless channels," *Electron. Lett.*, vol. 34, no. 9, pp. 851–852, Apr. 1998.
[4] P. Shankar, "Error rates in generalized shadowed fading channels," *Wireless Pers. Commun.*, vol. 28, no. 3, pp. 233–238, Feb. 2004.
[5] F. Yilmaz and M.-S. Alouini, "A new simple model for composite fading channels: Second order statistics and channel capacity," in *Proc. 7th ISWCS*, Sep. 2010, pp. 676–680.
[6] I. S. Ansari, M. M. Abdallah, M.-S. Alouini, and K. A. Qaraqe, "Outage performance analysis of underlay cognitive RF and FSO wireless channels," in *Proc. 3rd IWOW*, Sep. 2014, pp. 6–10.
[7] A. Jurado-Navas, J. M. Garrido-Balsells, J. F. Paris, and A. Puerta-Notario, *Numerical Simulations of Physical and Engineering Processes*. Rijeka, Croatia, InTech, 2011, ch. 8, pp. 181–206.
[8] B. Carter and M. Springer, "The distribution of products, quotients and powers of independent H-function variates," *SIAM J. Appl. Math.*, vol. 33, no. 4, pp. 542–558, Dec. 1977.
[9] J. I. D. Cook, "The H-function and probability density functions of certain algebraic combinations of independent random variables with H-function probability distribution," Ph.D. dissertation, Univ. Texas, Dept. Mech. Eng., Austin, TX, USA, May 1981.
[10] C. D. Bodenschatz, "Finding an H-function distribution for the sum of independent H-function variates," Ph.D. dissertation, Univ. Texas, Dept. Mech. Eng., Austin, TX, USA, May 1992.
[11] M. K. Simon and M.-S. Alouini, "A unified approach to the performance analysis of digital communication over generalized fading channels," *Proc. IEEE*, vol. 86, no. 9, pp. 1860–1877, Sep. 1998.
[12] M.-S. Alouini and A. Goldsmith, "A unified approach for calculating error rates of linearly modulated signals over generalized fading channels," *IEEE Trans. Commun.*, vol. 47, no. 9, pp. 1324–1334, Sep. 1999.
[13] G. Ropokis, A. Rontogiannis, P. Mathiopoulos, and K. Berberidis, "An exact performance analysis of MRC/OSTBC over generalized fading channels," *IEEE Trans. Commun.*, vol. 58, no. 9, pp. 2486–2492, Sep. 2010.
[14] R. Palat, A. Annamalai, and J. Reed, "An efficient method for evaluating information outage probability and ergodic capacity of OSTBC system," *IEEE Commun. Lett.*, vol. 12, no. 3, pp. 191–193, Mar. 2008.
[15] M. El Ayadi and M. Ismail, "Novel closed-form exact expressions and asymptotic analysis for the symbol error rate of single–and multiple-branch MRC and EGC receivers over $\alpha - \mu$ fading," *IEEE Trans. Veh. Techn.*, vol. 63, no. 9, pp. 4277–4291, Nov. 2014.
[16] R. B. Paris and D. Kaminski, *Asymptotics and Mellin–Barnes Integrals*. Cambridge, U.K.: Cambridge Univ. Press, 2001.

[17] K. Yao, M. Simon, and E. Bigileri, "Unified theory on wireless communication fading statistics based on SIRP," in *Proc. 5th IEEE Workshop Signal Process. Adv. Wireless Commun.*, Jul. 2004, pp. 135–139.

[18] Z. Ji, C. Dong, Y. Wang, and J. Lu, "On the analysis of effective capacity over generalized fading channels," in *Proc. IEEE ICC*, Jun. 2014, pp. 1977–1983.

[19] F. Yilmaz and M.-S. Alouini, "A novel unified expression for the capacity and bit error probability of wireless communication systems over generalized fading channels," *IEEE Trans. Commun.*, vol. 60, no. 7, pp. 1862–1876, Jul. 2012.

[20] S. Ekin *et al.*, "Achievable capacity of a spectrum sharing system over hyper fading channels," in *Proc. IEEE GLOBECOM*, Nov. 2009, pp. 1–6.

[21] A. Mathai, R. K. Saxena, and H. Haubold, *The H Function: Theory and Applications*. New York, NY, USA: Springer-Verlag, 2010.

[22] J. Berterand, P. Bertrand, and J.-P. Ovarlez, *The Transform and Applications Handbook*. Boca Raton, FL, USA: CRC, 1995.

[23] A. Kilbas, "Analytical methods and special functions," *H-Transforms: Theory and Applications*. New York, NY, USA: Taylor & Francis, 2004.

[24] I. S. Gradshteyn and I. M. Ryzhik, *Table of Integrals, Series and Products*. San Diego, CA, USA: Academic, 2000.

[25] A. Prudnikov, Y. A. Brychkov, and O. Marichev, *Integrals and Series: Special Functions*. New York, NY, USA: Gordon and Breach, 1986.

[26] F. Yilmaz and M.-S. Alouini, "Novel asymptotic results on the high-order statistics of the channel capacity over generalized fading channels," in *Proc. 13th IEEE Int. Workshop SPAWC*, Jun. 2012, pp. 389–393.

[27] H. M. Srivastava and R. Panda, "Some bilateral generating functions for a class of generalized hypergeometric polynomials," *J. Reine Angew. Math.*, vol. 1976, no. 283/284, pp. 265–274, Jan. 1976.

[28] F. Yilmaz and M.-S. Alouini, "A novel ergodic capacity analysis of diversity combining and multihop transmission systems over generalized composite fading channels," in *Proc. IEEE ICC*, Jun. 2012, pp. 4605–4610.

Husam R. Alhennawi received the B.Sc. degree in electrical engineering from the Islamic University of Gaza, Gaza, Palestine, in 2011 and the M.Sc. degree in electronics and communications engineering from Cairo University, Giza, Egypt, in 2014.

He is currently with the Department of Electronics and Electrical Communications Engineering, Faculty of Engineering, Cairo University. His research interests include cognitive radio networks and performance evaluation of digital communication systems.

Moataz M. H. El Ayadi (M'14) received the B.Sc. (Hons.) degree in electronics and communication engineering and the M.Sc. degree in engineering mathematics and physics from Cairo University, Giza, Egypt, in 2000 and 2004, respectively, and the Ph.D. degree in electrical and computer engineering from the University of Waterloo, Waterloo, ON, Canada, in 2008.

From 2000 to 2004, he was a Teaching Assistant with the Department of Engineering Mathematics and Physics, Faculty of Engineering, Cairo University. From 2004 to 2008, he was a Research and Teaching Assistant with the Center of Pattern Analysis and Machine Intelligence, University of Waterloo. From January 2009 to March 2010, he was also a Postdoctoral Research Fellow with the Multimedia Laboratory, The Edward S. Rogers Sr. Department of Electrical and Computer Engineering, University of Toronto, Toronto, ON, Canada. Since April 2010, he has been an Assistant Professor with the Department of Engineering Mathematics and Physics, Cairo University. From March 2012 to March 2014, he was a Senior Research Expert with Orange Labs, Cairo, Egypt. He is currently a Research Scientist with VoiceTrust eServices Inc., Toronto. His research interests include signal processing, performance analysis of digital communication systems, statistical pattern recognition, speech recognition, semantic analysis, natural language call routing, signal processing applications, machine learning, and speaker identification systems.

Dr. El Ayadi has served as a Reviewer for many peer-reviewed journals. He received Publication Awards from Cairo University in 2012 and 2013, as well as Faculty of Engineering Scholarships from the University of Waterloo in 2005 and 2007.

Mahmoud H. Ismail (S'00–M'07–SM'15) received the B.Sc. (Hons.) degree in electronics and electrical communications engineering and the M.Sc. degree in communications engineering from Cairo University, Giza, Egypt, in 2000 and 2002, respectively, and the Ph.D. degree in electrical engineering from The University of Mississippi, Oxford, MS, USA, in 2006.

From August 2000 to August 2002, he was a Research and Teaching Assistant with the Department of Electronics and Electrical Communications Engineering, Cairo University. From 2004 to 2006, he was a Research Assistant with the Center for Wireless Communications (CWC), University of Mississippi. From 2006 to 2014, he was also a Systems Engineering Consultant with Newport Media Inc. (now Atmel Corporation) Egypt Design Center, Giza. He is currently an Associate Professor with the Department of Electronics and Electrical Communications Engineering, Cairo University, and an Associate Professor with the American University of Sharjah, Sharjah, United Arab Emirates. His research interests include wireless communications, with emphasis on performance evaluation of next-generation wireless systems, communications over fading channels, and error-control coding.

Dr. Ismail has served as a Reviewer for several refereed journals and conferences. He received the University of Mississippi Summer Assistantship Award in 2004 and 2005, The University of Mississippi Dissertation Fellowship Award in 2006, The University of Mississippi Graduate Achievement Award in Electrical Engineering in 2006, and the Best Paper Award presented at the 10th IEEE Symposium on Computers and Communications, La Manga del Mar Menor, Spain. He is a member of the Sigma Xi and Phi Kappa Phi Societies.

Hebat-Allah M. Mourad received the B.Sc., M.Sc., and Ph.D. degrees from Cairo University, Giza, Egypt, in 1983, 1987, and 1994, respectively, all in communications engineering.

Since 1983, she has been with the Department of Electronics and Electrical Communications, Faculty of Engineering, Cairo University, where she is currently a Full Professor. From 2008 to 2012, she was the Director of the High Technology Center (HTC), Faculty of Engineering, Cairo University. From 2010 to 2012, she was also a member of the technical office of the postgraduate and research sector of Cairo University. Her research interests include wireless communications, cognitive radio, and next-generation cellular networks.

Dr. Mourad has been named in *Marquis Who's Who in Science and Engineering* since the year 2004.